THE EFFECTS OF HYDROGEN, HYDROGEN SULFIDE, AND AMMONIA ON THE ELEVATED TEMPERATURE DETERIORATION OF METALS AND ALLOYS IN CARBONACEOUS GAS ENVIRONMENTS

A THESIS

Presented to

The Faculty of the Graduate Division

by

Harry Marshall Thron, Jr.

In Partial Fulfillment

of the Requirements for the Degree

Master of Science in Metallurgy

Georgia Institute of Technology

September, 1968

In presenting the dissertation as a partial fulfillment of the requirements for an advanced degree from the Georgia Institute of Technology, I agree that the Library of the Institute shall make it available for inspection and circulation in accordance with its regulations governing materials of this type. I agree that permission to copy from, or to publish from, this dissertation may be granted by the professor under whose direction it was written, or, in his absence, by the Dean of the Graduate Division when such copying or publication is solely for scholarly purposes and does not involve potential financial gain. It is understood that any copying from, or publication of, this dissertation which involves potential financial gain will not be allowed without written permission.

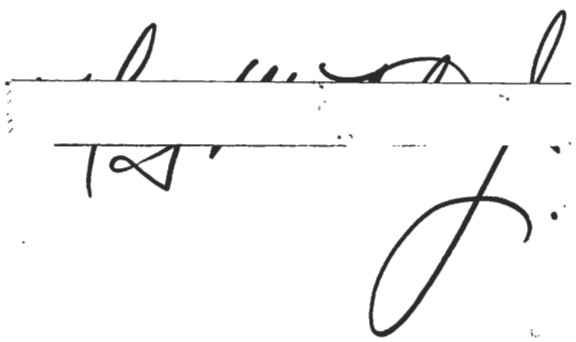

7/25/68

THE EFFECTS OF HYDROGEN, HYDROGEN SULFIDE, AND AMMONIA ON THE ELEVATED TEMPERATURE DETERIORATION OF METALS AND ALLOYS IN CARBONACEOUS GAS ENVIRONMENTS

Approved: _____

_____
Chairman

_____

_____

_____

Date approved by Chairman: 11/15/68

ACKNOWLEDGMENTS

I would like to express appreciation to my faculty advisor, Dr. R. F. Hochman, and to my reading committee, Dr. N. N. Engel and Dr. H. V. Grubb, for their assistance and suggestions.

My sincere appreciation is extended to Texaco, Incorporated, for the provision of a Research Fellowship and to Mr. S. O. Fernandez who, as a Texaco representative, expressed a personal interest in my work. I am also grateful for the experimental gases provided by the Linde Division, Union Carbide Corporation.

TABLE OF CONTENTS

TABLE OF CONTENTS (continued)

LIST OF TABLES

LIST OF FIGURES

LIST OF FIGURES (continued)

LIST OF FIGURES (continued)

LIST OF FIGURES (continued)

SUMMARY

The purpose of the research was to determine the behavior of selected metals and industrial alloys in carbonaceous gas atmospheres containing hydrogen. Coiled wire samples of pure iron, cobalt, nickel 200, Inconel 600, and AISI types 302, 316, and 416 stainless steel were subjected to atmospheres containing pure carbon monoxide, 5 and 10% hydrogen in carbon monoxide, pure methane, and 5% hydrogen in methane. Specimens were exposed to the various environments at temperatures ranging from 500° to 900°C for a period of 20 hours. Previous research has shown that 20 hours is the optimum duration of reactivity experiments. In addition, limited studies were conducted with atmospheres of pure hydrogen sulfide and pure ammonia to determine the inhibitive characteristics of these gases.

Results of studies with carbon monoxide and hydrogen-carbon monoxide atmospheres indicated that iron, cobalt, nickel 200, and 416 stainless steel were more reactive in hydrogen-containing environments than in pure carbon monoxide; whereas, types 302 and 316 stainless showed highest reactivity in pure carbon monoxide. Inconel 600 exhibited least reactivity in the 10% H_2-CO environment. Nickel 200, Inconel 600, and the 300 series stainless steels showed the best overall resistance to attack in H_2-CO atmospheres, while iron was the most reactive of the materials tested.

Studies with pure methane and 5% hydrogen in methane revealed that iron reacted similarly in both pure and mixed atmospheres. Types

302 and 316 stainless showed increasing reactivity with increasing temperature above 750°C. In pure methane, 416 stainless, cobalt, and Inconel 600 showed low temperature reaction peaks at 700°C, 750°C, and 775°C, respectively. Nickel 200 exhibited reactivity maxima at 700°C and 800°C in 5% H_2-CH_4 and pure CH_4, respectively. Cobalt and 416 stainless steel were, by far, the least reactive of all the materials tested in the hydrocarbon atmospheres, while Inconel 600 showed the most reactivity.

From the reactivity studies it was concluded that: (1) hydrogen in carbon monoxide promotes carbon deposition and surface attack in all the materials except the 300 series stainless steels, (2) hydrogen does not significantly affect the reactivity of methane with iron-base alloys, and (3) the reactivity of the various metals and alloys in methane becomes significant only at temperatures above 650°C, the minimum temperature for the initiation of the thermal decomposition of methane to carbon and hydrogen.

Pretreatment of samples with ammonia substantially inhibited carbon deposition for iron and types 302 and 316 stainless steel. Samples of iron, cobalt, and type 416 stainless steel pretreated with hydrogen sulfide exhibited improved resistance to deterioration compared to samples with no pretreatment.

Scanning electron micrographs (SEM) of surface deposits revealed distinct structural differences among samples reacted in carbon monoxide and methane environments. Optical microscopy provided information about the chemical composition and distribution in selected samples.

CHAPTER I

INTRODUCTION

The deterioration of metals and alloys at elevated temperatures in carbonaceous environments is commonly known as metal dusting. Perhaps the principal reason for the recent emphasis on metal dusting research lies in its deleterious effects on existing or potential industrial processes (1). Certain hydrocarbon syntheses are subject to carbon deposition with subsequent blockage of the reaction vessel and deactivation or disintegration of the catalysts. For example, a plant designed to convert coal to gasoline and various other petrochemicals experienced severe metal deterioration in atmospheres containing carbon dioxide and hydrogen. Nuclear reactors with graphite moderators using carbon dioxide coolants may experience carbon monoxide formation in the high temperature reactor zone and carbon monoxide decomposition to carbon in the low temperature zone.

The commercial utility of the carbon deposition reaction was shown during World War II when the Germans used the reaction to produce a substitute for carbon black (2). Several patents have been awarded for processes involving the decomposition of carbon monoxide. A French patent describes the production of carbon in a falling-bed reactor using a finely divided iron catalyst (1,3). A more recent United States patent concerns apparatus for the production of carbon black under special conditions in the absence of a metallic catalyst (4).

Carbon monoxide and hydrocarbon atmospheres have been extensively studied with respect to their effects on ferrous and non-ferrous materials commonly used in industrial processes, but the first comprehensive attempt to evaluate metal dusting wastage came in 1959 when the National Association of Corrosion Engineers devoted an entire session to the deterioration reactions in carbonaceous environments (5).

To analyze the deterioration effectively, it was expedient to limit the variables in the metal dusting system. Therefore, previous basic research has dealt primarily with pure metals in pure carbon monoxide or hydrocarbon environments. A logical extension of this work is to investigate the effects of alloying elements on the reaction or to determine the changes in reaction characteristics caused by mixed gases. The presence of hydrogen in carbon monoxide and hydrocarbon systems is so common that an evaluation of its effects on the metal dusting reaction should prove to be of considerable practical importance. This study will be an attempt to determine the effects of hydrogen on the dusting characteristics of some commercially-important metals and alloys in carbon monoxide and methane environments.

CHAPTER II

LITERATURE SURVEY

Reaction of Carbonaceous Gases with Iron and Cobalt

It is generally accepted that the carbon deposition reaction (Boudouard Reaction)

$$2CO \rightarrow CO_2 + C$$

proceeds at significant rates only in the presence of a catalyst. Iron, nickel, and cobalt are found to be the most active catalysts (6). Although from the literature the precise nature of the catalysis is not clear, it has been shown that treatment of the carbided base metal with hydrogen decomposes some of the carbide with production of methane and regeneration of the base metal (7). For example, hydrogen has been shown to alter the characteristics of carbon formation from carbon monoxide over iron catalysts. Walker, Rakszawski, and Imperial (1) suggest that hydrogen reactivates iron by converting the carbide (Fe_3C) to iron. The conversion proceeds as carbon monoxide adsorbs and dissociates on the iron. Liberated carbon atoms migrate to a nucleating center where cementite (Fe_3C) is formed. Formation of cementite retards CO decomposition but treatment with hydrogen reactivates the catalyst for further carbon production (8). X-ray diffraction studies confirm that the major constituent of a spent catalyst is cementite. Hydrogen has a similar effect on cobalt, although the cobalt-substituted

cementite is less stable than the iron (9). This regenerative effect of hydrogen has been confirmed by several investigators (8,9,10). Furthermore, hydrogen is commonly used to reduce oxides in catalyst preparation.

Westerman (11) studied the mechanism and kinetics of iron deterioration in carbon monoxide. Iron wire samples experienced maximum weight gains at about 570°C. Reactivity decreased to a minimum at 710°C and a gradual increase in reaction was noted with increasing temperature from 710°C to 1000°C. The mechanism postulated for carbon monoxide decomposition in the alpha-iron region was as follows: (1) adsorption of carbon monoxide on ferrite, (2) Boudouard reaction ($2CO \rightarrow CO_2 + C$) releasing carbon, (3) formation of cementite, and (4) decomposition of cementite to iron and graphite.

Walker, et al. (1), studied carbon formation from carbon monoxide-hydrogen mixtures over iron catalysts. Results indicated that for gas mixtures containing less than 40 per cent hydrogen, extraneous reactions producing methane have relatively little effect on the true picture of carbon deposition. The temperature at which the maximum rate of carbon deposition occurred increased with increasing hydrogen content. Furthermore, increasing hydrogen content was found to markedly increase the amount of carbon which could be formed from a given catalyst weight.

Hofer (12) investigated the formation of free carbon over a cobalt-thoria-kieselguhr catalyst. It was proposed that carbon formation over cobalt follows two routes, namely, a surface process, and a process involving a carbide intermediate. This result was based on

studies of two catalyst specimens, identical except that the cobalt in one had been converted to Co_2C by carburization with carbon monoxide. Carbon deposition was initially twenty times faster on the metallic catalyst than on the carbided catalyst. During carburization the rate of carbon deposition on the metallic catalyst decreased considerably, whereas the rate on the carbided catalyst remained constant. It was concluded that the carbide inhibited the deposition of carbon similar to the carbide of iron, but unlike iron carbide, cobalt carbide was considered partially active to carbon formation.

Iron and cobalt appear to actively promote carbon monoxide decomposition and follow basically similar reaction mechanisms. Iron, however, experiences considerably more carbon deposition than cobalt.

Reaction of Carbonaceous Gases with Stainless Steels

Hoyt and Caughey (13) studied the effects of gases containing carbon monoxide and hydrogen on stainless steels. Gases containing from 12 to 20% carbon monoxide were found to attack type 310 stainless steel at about 1200°F. The severe pitting and metal loss observed was attributed principally to carburization. Chemically active carbon formed by the decomposition of carbon monoxide combined with the metal to form a carbide which could be lifted from the surface by carbon deposits and transported into the gas stream.

Segraves (14) investigated the corrosive effects of carbon monoxide on 304 stainless steel from 920° to 1100°F at atmospheric pressure and for times ranging from 4 to 120 hours. His experiments showed a temperature dependency from 900° to 1100°F for 16-hour

exposures to carbon monoxide. Analyses of surface deposits were inconclusive. Segraves concluded that the reaction of 304 stainless steel with carbon monoxide was temperature dependent, that most reaction occurred above 1020°F, and finally that in polycrystalline 304 stainless, grain boundary attack led to localized failure.

Phillips, et al. (15), found that the failure of 304 stainless steel tubes in a butadiene cracking operation occurred by metal dusting phenomena. The tubes exhibited severe carburization and pitting with a uniform surface attack. Low sulfur concentrations, up to about 0.5%, showed good inhibitive characteristics. Carbon disulfide, mercaptans, and free sulfur were the chief forms present.

Burns (16) reported severe corrosion in a system containing low sulfur crude. Although the deterioration was attributed to iron sulfide, the presence of carbon deposits afforded the possibility of metal dusting. Merrick (17) reported that certain nickel-chromium steels experienced heavy pitting above 750°C. In this instance the sulfur present did not affect the corrosion rate of type 309 stainless steel. In more general investigations of iron-nickel-chromium alloys in atmospheres containing CO, CO_2, H_2, and H_2O, several forms of attack were found (18). Heavy carbon deposition, internal oxidation, and severe pitting have all been observed. Hubbel (19) also found that certain stainless steel aircraft exhaust manifolds experienced carbon monoxide attack at elevated temperatures.

Phillips Petroleum Company (20) tested various stainless steels in an effort to alleviate corrosion problems in the production of butenes by catalytic dehydrogenation of butane. The following types

of steels were tested on plant scale equipment: AISI 302B, 316, 304, 321, 310, and 347. Of these, only types 302B, 310, and 316 gave satisfactory results; e.g., operated without plugging the reactor with reaction products. Type 316 yielded the greatest amount of carbon formation of the materials tested.

In summary, stainless steels show various types of deterioration in carbonaceous gases, although the attack is usually of smaller magnitude than for iron and cobalt. The reaction of carbon-bearing gases with stainless steels is often characterized by internal carburization and carbide formation.

Reaction of Carbonaceous Gases with Nickel-Base Alloys

Segraves (14) also investigated the corrosive tendencies of carbon monoxide on pure nickel and Inconel from 920°F to 1100°F and atmospheric pressure. Experimental results were limited, but definite weight increases from carbonaceous reaction products were noted.

Cox (21) found that pure nickel did not react with, nor catalyze the decomposition of carbon monoxide at 1200°F for reaction times up to 45 minutes. Nickel oxide was reduced to pure nickel by carbon monoxide at 1200°F without accompanying reactions. Pure nickel obtained from reduction by carbon monoxide did not catalyze the decomposition reaction, but nickel obtained from reduction by hydrogen did. The explanation offered for these phenomena was that hydrogen absorbed on the nickel crystallites reduced the carbon monoxide.

Kehrer and Leidheiser (22) investigated the decomposition of carbon monoxide catalyzed by nickel single crystals. Regions surrounding

the (111) faces of the crystals were found to be the most active catalytic areas. X-ray diffraction and chemical analysis confirmed the presence of nickel and carbon in the surface deposits. In addition, Grenga (23) used electron microscopy to show that the order of decreasing regions of activity on thin films for the decomposition reaction was (111) > (110) > (100).

Skinner and Raudebaugh (24) subjected a number of metals to carbon monoxide from 1000° to 1200°F. Annealed strips of Inconel and Incoloy were exposed to CO for 70 hours, but the experiments failed to show any carbonaceous deposits, neither in the reaction zone, nor on the surface of the metal specimens. In addition, specimens of Inconel and Incoloy were simultaneously exposed with gray iron at 1050°F in an attempt to induce reaction in the previously unaffected materials. Neither of the samples was attacked.

Nickel-base alloys promote appreciable carbon deposition only at temperatures considerably above those where ferrous alloys experience maximum deposition. Furthermore, the reaction of CO with nickel is found to be a selective process involving decomposition of CO on certain crystallographic regions.

Survey of the Effects of Carbonaceous Gases on Metals and Alloys

From tests on numerous steels and industrial alloys, it appears that the materials most resistant to dusting are those most resistant to carburization (25), i.e., nickel, monel, or Inconel. Chromium-containing steels exhibit sufficient resistance for satisfactory operation under certain conditions in the petroleum industry. Silicon and

molybdenum increase the dusting resistance of the 18-8 types of stainless steels (26).

Segraves (14) summarized the work of Baukloh and Hieber (27) who studied the catalytic activity of numerous materials in carbon monoxide environments. A condensation of Segraves' summary is as follows:

Material	Temperature of Maximum Carbon Deposition, °C	Maximum Deposition in 1/2 Hour, Grams
Fe	550	0.40
Co	650	0.15
Ni	750	0.15
Mn	850	0.02
Cr	650	0.005
Al	550	0.002
Cu	---	no appreciable deposition

It has also been shown that small amounts of hydrogen in methane significantly affected the reactivity of certain commercial alloys (28). Inconel and hastelloy, for example, show lower temperatures of maximum reactivity and less carbon deposition and carburization when exposed to a methane - 1.7 per cent hydrogen atmosphere. This small percentage of hydrogen does not appear to affect the reaction of methane with types 302 or 304 stainless steel and Incoloy 800.

Hydrogen in carbon monoxide (CO - 1.92 per cent H_2) appears to raise the temperature of maximum reactivity of iron and lower the temperature for significant reaction in nickel. The reactivity of cobalt becomes appreciable at higher temperatures in the gas mixture than in pure carbon monoxide. Three hundred series stainless steels

exhibit reactivity peaks at lower temperatures in the hydrogen-carbon monoxide mixture while Inconel 600 shows an increase in reactivity at higher temperatures (29).

Thus, the extent of deterioration is affected by several factors including alloy and gas compositions, and the temperature of reaction. This study will be an attempt to evaluate the effects of alloying elements and mixed gases on the metal dusting reactions at various temperatures.

Inhibitors to the Reaction of Metals and Alloys with Carbonaceous Gases

Several processes, stemming from costly industrial experiences, have been developed to inhibit the harmful effects of the metal dusting reactions. The steel industry has long been plagued with problems arising from carbon formation. As early as 1876 Pattinson (30) suggested that small quantities of iron embedded in the furnace brick catalyzed carbon deposition which subsequently disintegrated the firebrick. Shea (31) showed that blast furnace bricks could be protected against carbon monoxide attack by treatment with sulfuric acid, ammonium and aluminum sulfates, and hydrogen sulfide gas. Various other compounds containing sulfur and chlorine were also found to be effective.

Burns (16) used ammonia injection to neutralize the corrosive elements in the furnace tubes of a distillation unit processing low sulfur crude oil. Selected nitrogen compounds such as cyanogen have also been shown to retard the carbon deposition (32,33).

Hochman (34) described a method whereby a 25% chromium steel

showed improved metal dusting resistance in an atmosphere of methane and hydrogen after pretreatment with a low partial pressure of oxygen. The improved corrosion resistance was attributed to the formation of an oxide which was thermodynamically stable to attack by the carbonaceous environment. Preoxidation of alloys containing silicon and aluminum have shown similar favorable results.

The petroleum industry has been classically concerned with the problems of metal dusting. Equipment for processing crude oil is most susceptible to the decomposition reactions. Sulfur in the crude has been identified as a principal factor in the corrosion process, but sulfur content alone is not an accurate indication of the corrosion potential.

Furnace tubes of 18-8 type stainless steels have been successfully used in high temperature petroleum cracking operations, although the tubes were exposed to extremely corrosive environments. Camp, et al. (15), however, discussed a unique case of severe hydrocarbon-side corrosion of 18-8 stainless furnace tubes. The attack occurred in a superheater furnace where naptha was cracked in the vapor phase for production of butadiene. Tests to determine the effects of various sulfur compounds on the tendency of the naptha to corrode the 18-8 alloy in the temperature range 1300° to 1500°F showed that the addition of sulfur (as free sulfur, butyl mercaptan, or carbon disulfide) effectively eliminated the corrosicn. Results also indicated that amounts lower than 0.05% sulfur markedly reduced corrosion, but that more consistent effects were possible upon additions of 0.05% and higher of sulfur.

Additions of water in amounts ranging from 0.06 to 0.4% were also found to eliminate the corrosion. Larger additions of water were not detrimental, but were necessary. Furthermore, water was found to substantially reduce the tendency of the furnace tubes to coke. Under other conditions, however, researchers (35) have found that water may accelerate the corrosion process. Further tests by Camp, et al., (15) indicated that carbon dioxide, ethanol, acetic acid, hydrogen sulfide, and sulfur dioxide were satisfactory inhibitors for the particular type of corrosion experienced in the cracking operation.

Hence, numerous techniques are available to alleviate metal dusting wastage with the desirability of any given inhibitor determined by the characteristics of the particular system under consideration. Ammonia injection, for example, would be a poor choice for elimination of corrosion in a system containing copper.

CHAPTER III

EXPERIMENTAL APPARATUS AND PROCEDURE

Material

To determine the reactivities of typical industrial metals and alloys in the carbonaceous environments, the following materials were used: pure iron, pure cobalt, nickel 200, 302 stainless steel, 316 stainless steel, 416 stainless steel, and Inconel 600. Reaction gas atmospheres used included pure carbon monoxide, 5% hydrogen in carbon monoxide, 10% hydrogen in carbon monoxide, pure methane, and 5% hydrogen in methane. Physical and chemical characteristics of all the materials used in the study appear in Tables 8, 9, and 10 of Appendix A. In addition, pure hydrogen sulfide and pure ammonia were used to pretreat samples subsequently reacted in pure carbon monoxide.

Sample Preparation

All specimens used for the reactivity studies were in the form of wire coils of 10 cm^2 surface area. Other physical characteristics of the wires are given in Table 8 of Appendix A. The samples were prepared by winding a precut length of wire around a teflon mandrel of 0.25" diameter. After coiling, the specimens were cleaned in trichloroethylene prior to initial weighing.

Standard metallographic procedure was used to prepare samples for optical microscopy. No special preparation was required for examination of surface reaction products with the scanning electron microscope (SEM).

Apparatus

The principal experimental equipment used included the following:

(1) Lindberg horizontal tube furnace; 2" diameter; range: 0 - 1300°C; Controller with platinel No. 2 thermocouple

(2) Quartz glass furnace tube; 2" diameter x 3' long with appropriate pyrex ends

(3) Seven 9/16" diameter x 4" long quartz glass reaction tubes forming a hexagonal cluster

(4) Two Brooks-mite purge meters; model 2001-V; range: 0 - 0.08 scfh

(5) Airco rotameter; model 09-1021

Figures 1 and 2 show the experimental apparatus and reaction tube cluster, respectively. The cluster was designed to insure uniform gas flow over the specimens and to allow the seven specimens to be positioned equidistant from the gas inlet of the furnace.

Procedure

The reactivities of the seven materials tested were determined by gravimetric methods. After cutting, coiling, and cleaning, the seven materials were individually weighed on a Mettler balance, simultaneously subjected to the gas atmospheres in separate reaction tubes, and reweighed. The weight change of a particular material, including carbon deposits, after exposure to the carbonaceous atmosphere for a period of 20 hours was considered indicative of its reactivity. Previous studies[11] have shown that 20 hours is the optimum duration of

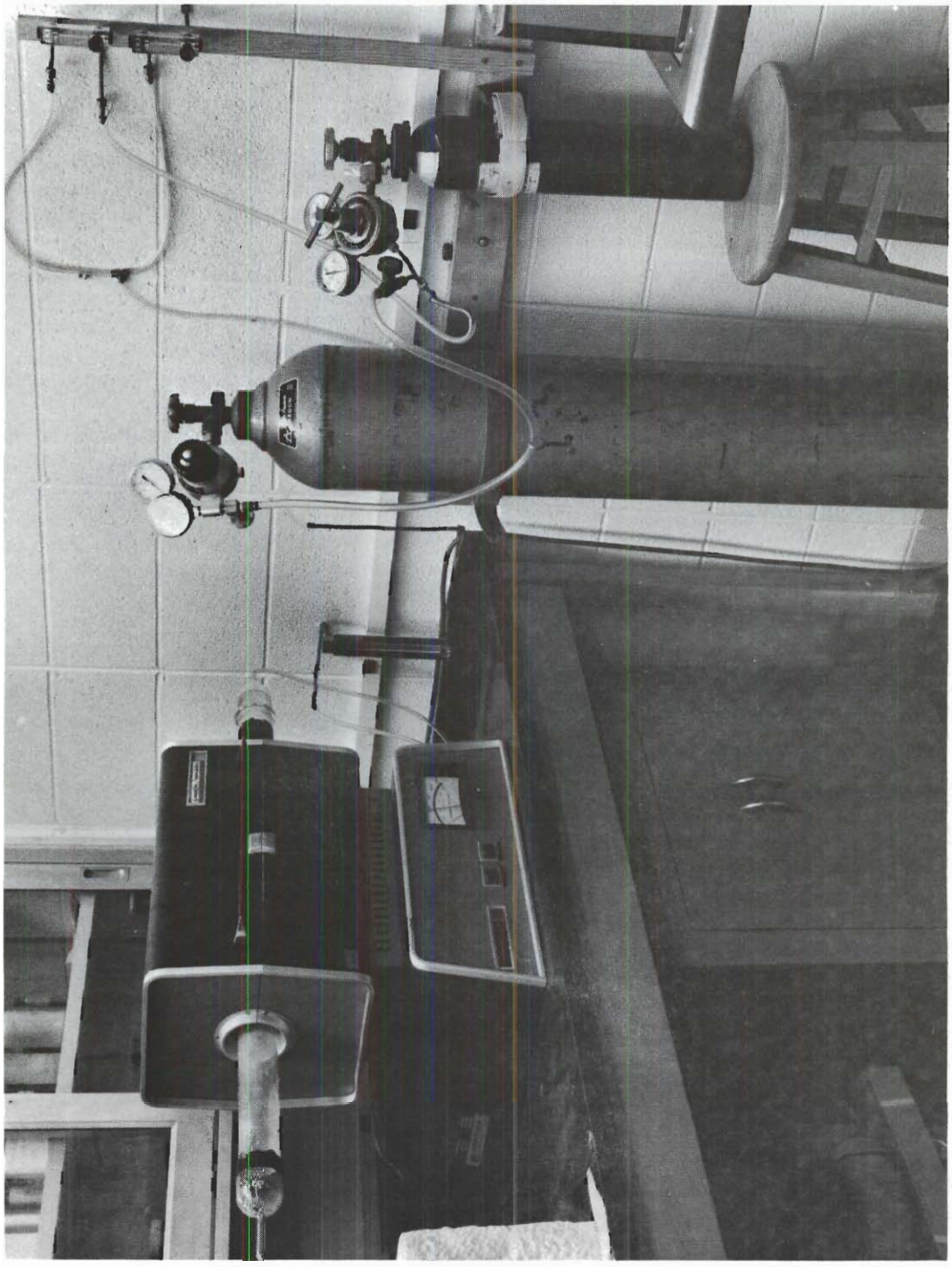

Figure 1. Experimental Apparatus.

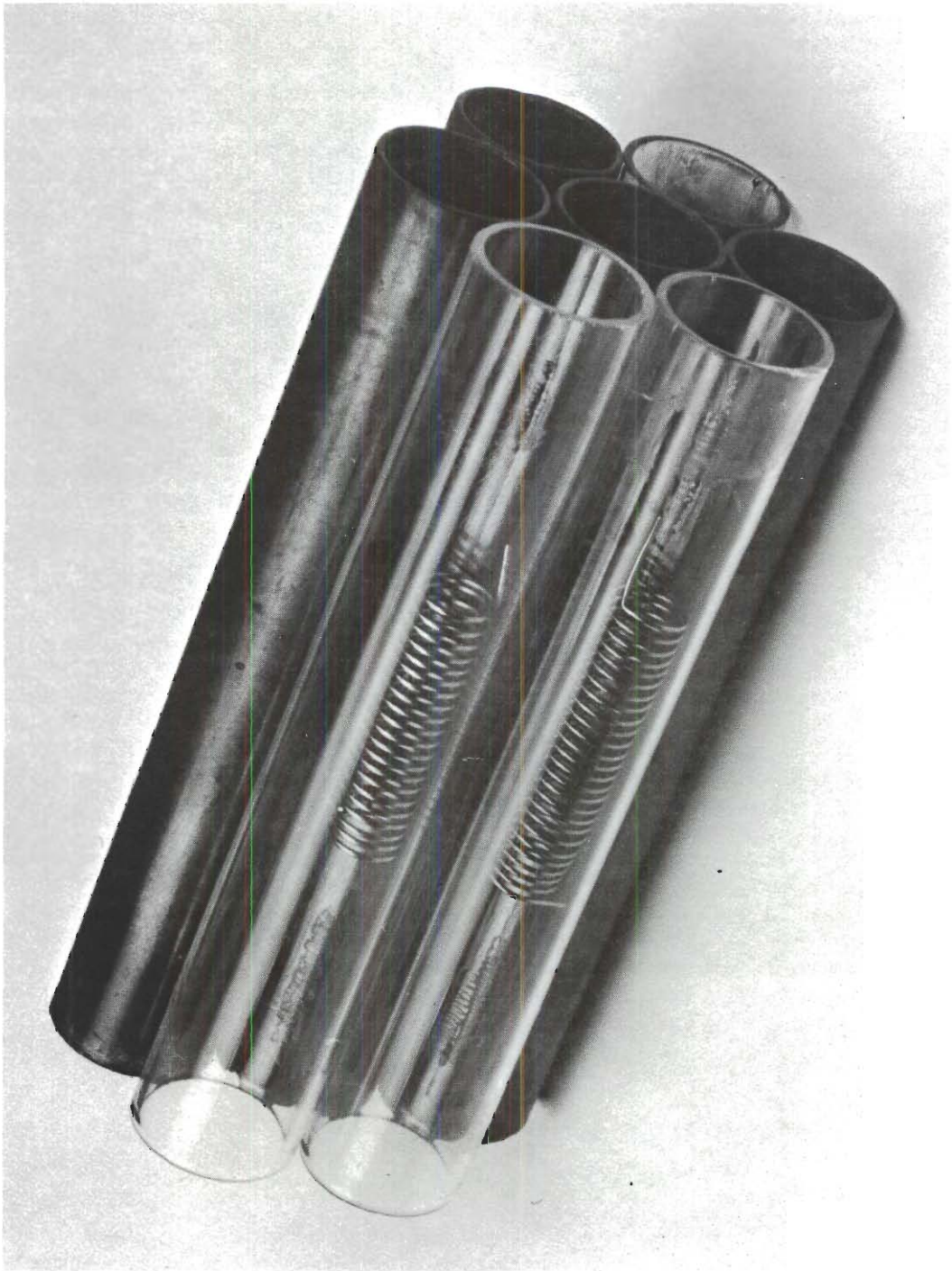

Figure 2. Reaction Tube Cluster.

reactivity experiments. A summary of the results of the reactivity studies appears in Tables 4 and 5.

The experimental procedure was as follows:

(1) Samples cut, coiled, cleaned, and weighed

(2) Samples positioned in reaction tubes

(3) Reaction tube cluster positioned in furnace

(4) System flushed with argon

(5) Furnace brought to temperature under inert atmosphere

(6) Reaction gas introduced

(7) Gas flow rate adjusted by rotameters to 15cc per minute

(8) Samples reacted for 20 hours

(9) System flushed with argon

(10) Furnace cooled under inert atmosphere

(11) Samples reweighed

In addition, several samples were pretreated with ammonia and hydrogen sulfide in attempts to inhibit the metal dusting reaction. The pretreatment temperatures were those where the particular materials experienced maximum reactivity in pure CO. Samples treated with ammonia were exposed for two hours at 650°C in 0.1 atm NH_3 and later reacted for twenty hours at 650°C in pure CO. Specimens treated with hydrogen sulfide were exposed for one hour at 550°C in 0.1 atm H_2S and subsequently reacted for twenty hours at 550°C in pure CO. Following the pretreatment the procedure used was identical to steps numbered (4) through (11) above. Results of the pretreatment studies appear in Tables 6 and 7.

CHAPTER IV

DISCUSSION OF RESULTS

The results of the deterioration studies can be best considered by dividing the experimental work into three general categories, namely, carbon monoxide-hydrogen, methane-hydrogen, and inhibitors. The results of experiments performed in carbon monoxide-hydrogen atmospheres will be considered first.

Carbon Monoxide-Hydrogen Mixtures

Reactivity Studies

An example of the reactivity experienced in the CO-H_2 gas system appears in Figure 3. The figure shows a comparison of reacted and unreacted iron samples. The specimen was reacted in 5% H_2-CO at 550°C for 20 hours and experienced extensive carbon deposition. The relative reactivities of the seven materials in 5% H_2-CO are shown in Figure 4. Iron, cobalt, and 416 stainless steel exhibited considerably more deposition than nickel 200, Inconel 600, and the 300 series stainless steels. A complete summary of the results of the reactivity studies, including the relative reactivities of the materials examined, appears in Tables 4 and 5. Previous research[11] has established the behavior of these materials in pure carbon monoxide, therefore, this study dealt primarily with the effects of hydrogen on their reactions in carbon monoxide atmospheres. However, experiments were also conducted in pure

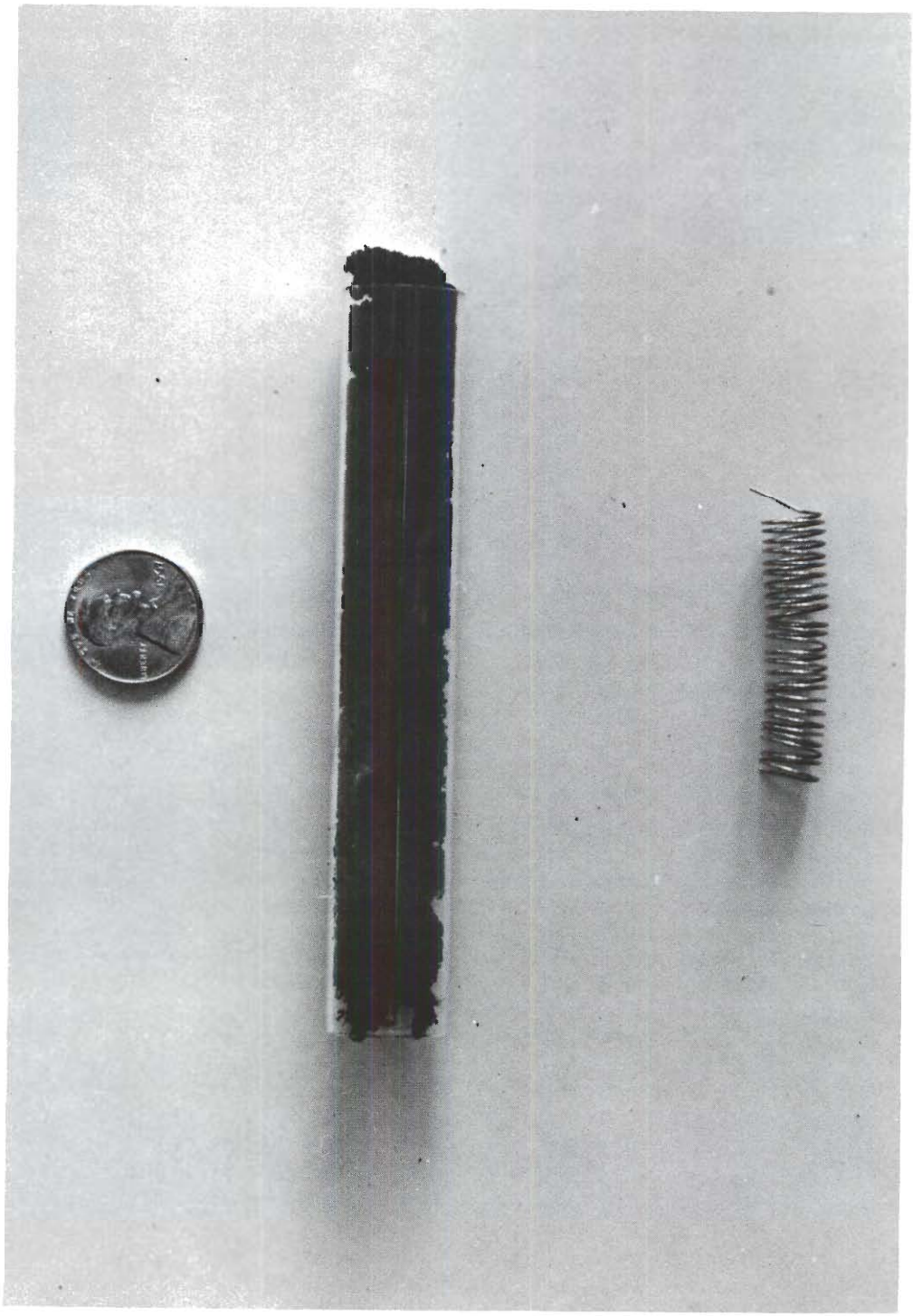

Figure 3. Comparison of Reacted and Unreacted Iron Samples; 5% H_2-CO, 550°C, 20 Hours.

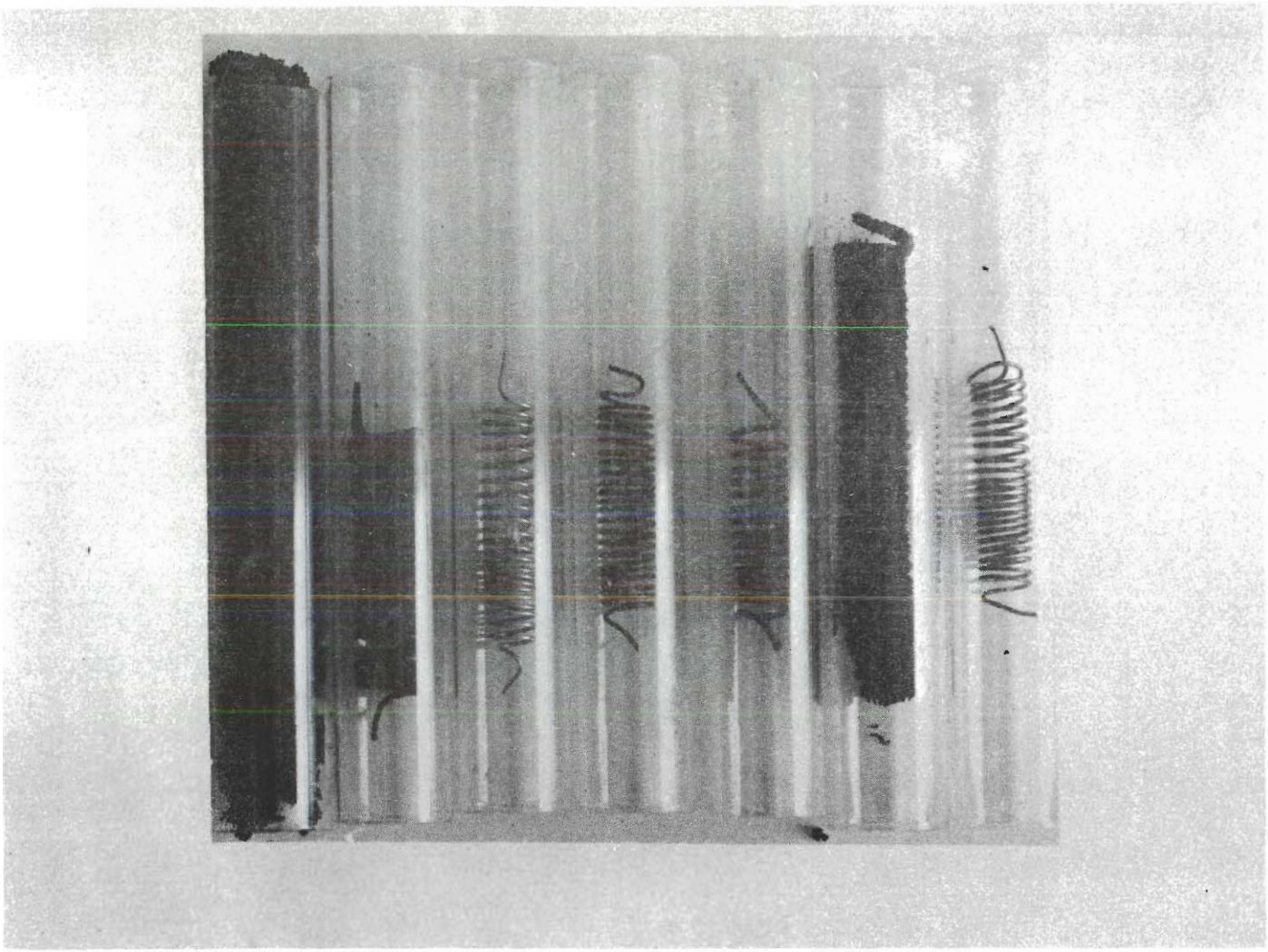

Figure 4. Comparison of Samples Reacted in 5% H_2-CO Atmosphere at 550°C for 20 Hours; L to R iron, cobalt, nickel 200, 302 SS, 316 SS, 416 SS, Inconel 600.

CO to establish a common basis for comparison between pure and mixed atmospheres.

The effect of hydrogen on the reaction of pure iron with carbon monoxide is shown in Figure 5. Iron reacted in 5% H_2-CO showed an increase in reactivity at low temperatures as compared to samples reacted in pure carbon monoxide. An increase in hydrogen content to 10% H_2-CO produced a significant decrease in reactivity indicating that the reaction was being inhibited.

The chemical reactions which may occur in carbon deposition systems containing C, CO, CO_2, H_2, H_2O, CH_4, and Fe appear in Table 1. It is well established, however, that the reactions which must be considered reduce to the following:

(1) $Fe + H_2O \rightleftarrows FeO + H_2$

(2) $3Fe + 4H_2O \rightleftarrows Fe_3O_4 + 4H_2$

(3) $Fe + CO_2 \rightleftarrows FeO + CO$

(4) $3Fe + 4CO_2 \rightleftarrows Fe_3O_4 + 4CO$

(5) $2CO \rightleftarrows CO_2 + C$ (Boudouard reaction)

(6) $CO + H_2 \rightleftarrows H_2O + C$

(7) $CO + H_2O \rightleftarrows CO_2 + H_2$ (Water-gas shift)

Carbide formation equilibria need not be considered since the carbide represents an intermediate and must always exist if free carbon is produced (6). If reactions involving methane are taken into account, their effects on the equilibrium are negligible; hence, the reactions pertinent to the thermodynamic analysis reduce to those numbered (1)

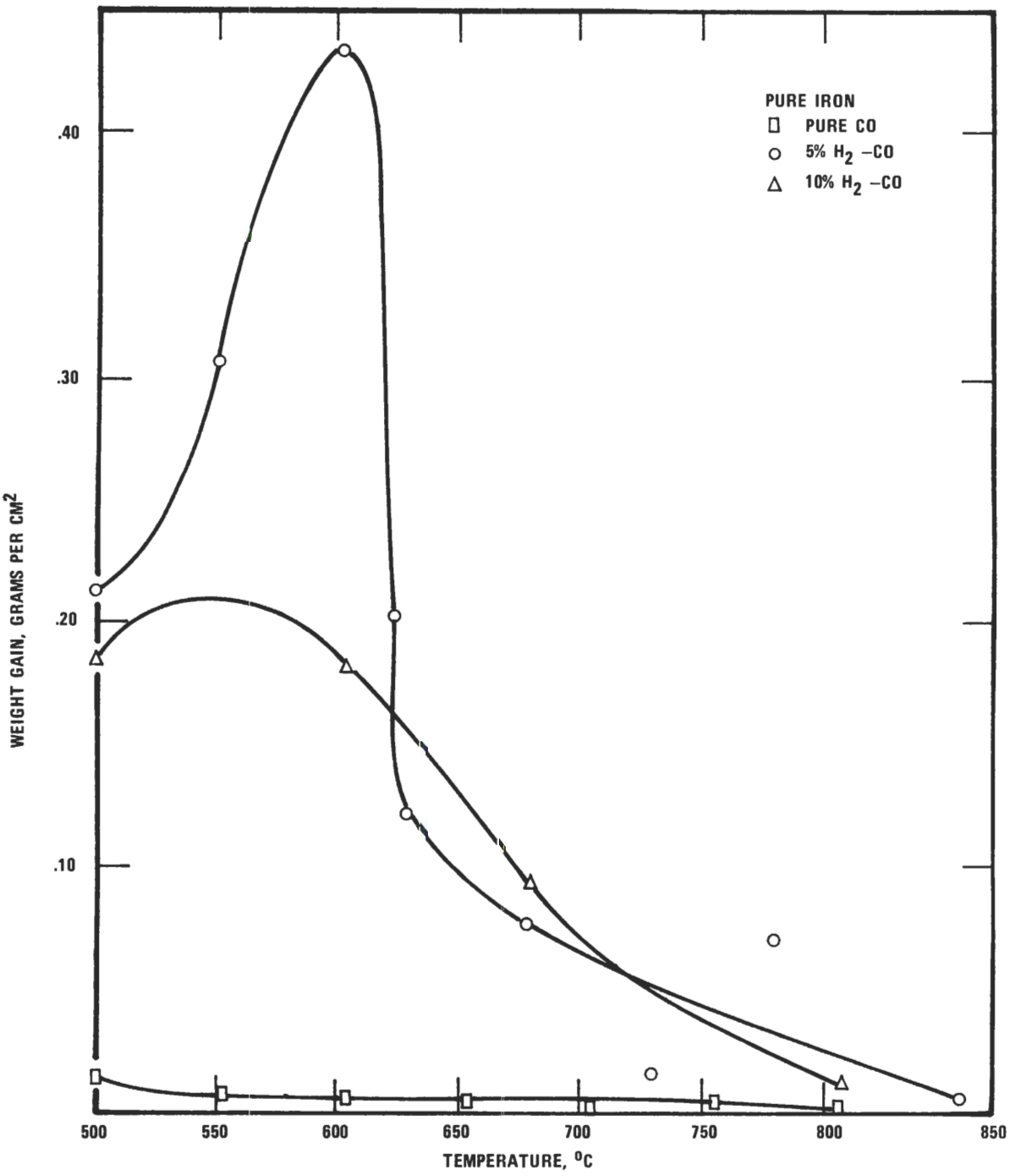

Figure 5. The Reactivity of Pure Iron in Pure CO, 5% H_2-CO, and 10% H_2-CO Environments.

Table 1. Chemical Reactions and Equilibria in the Carbon Deposition System

Reaction		Equilibrium Relationships						
1.	(a)		$Fe + H_2O$	$\rightleftarrows$	$FeO + H_2$		$K_1 = \frac{P_{H_2}}{P_{H_2O}}$
	(b)		$3Fe + 4H_2O$	$\rightleftarrows$	$Fe_3O_4 + 4H_2$		
2.	(a)		$Fe + CO_2$	$\rightleftarrows$	$FeO + CO$		$K_2 = \frac{P_{CO}}{P_{CO_2}}$
	(b)		$3Fe + 4CO_2$	$\rightleftarrows$	$Fe_3O_4 + 4CO$		
3.	(a)		$3Fe + 2CO$	$\rightleftarrows$	$Fe_3C + CO_2$		
	(b)	$3Fe +$	$CO + H_2$	$\rightleftarrows$	$Fe_3C + H_2O$		
	(c)		$3Fe + CH_4$	$\rightleftarrows$	$Fe_3C + 2H_2$		
4.	(a)		$C + CO_2$	$\rightleftarrows$	$2CO$		$K_4 = \frac{P_{CO} \times P_{CO}}{P_{CO_2}}$
5.	(a)		$C + H_2O$	$\rightleftarrows$	$CO + H_2$		$K_5 = \frac{P_{H_2} \times P_{CO}}{P_{H_2O}}$
6.	(a)		$CO + H_2O$	$\rightleftarrows$	$CO_2 + H_2$		$K_6 = \frac{P_{H_2} \times P_{CO_2}}{P_{H_2O} \times P_{CO}}$
7.	(a)		$C + 2H_2$	$\rightleftarrows$	CH_4		
	(b)		$CO + 3H_2$	$\rightleftarrows$	$CH_4 + H_2O$		
	(c)		$Fe_3C + 2H_2$	$\rightleftarrows$	$3Fe + CH_4$		

through (7) above. Equilibrium data for the reactions appear in Table 2.

For low hydrogen concentrations it is proposed that the Boudouard reaction, (4a), predominates. If the metal, not the carbide, is the catalyst, then any process creating iron surface area should increase the reactivity. Hydrogen and cementite, Fe_3C, are known to react as follows (1,8,9,10):

$$(3a) \qquad 3Fe + 2CO \rightleftarrows Fe_3C + CO_2$$

$$(3b) \qquad 3Fe + CO + H_2 \rightleftarrows Fe_3C + H_2O$$

$$(7a) \qquad 2H_2 + Fe_3C \rightleftarrows CH_4 + 3Fe$$

Thus, the presence of hydrogen allows regeneration of the base metal and results in increased catalytic surface and more reactivity. As the concentration of hydrogen in the system is increased, alternate reactions appear to become important. In addition to reaction (4a), the following reactions may occur:

$$(5a) \qquad CO + H_2 \rightleftarrows H_2O + C$$

$$(6a) \qquad CO + H_2O \rightleftarrows CO_2 + H_2$$

Everett (6) suggests that both reactions (4a) and (6a) contribute to the formation of carbon dioxide in the presence of high concentrations of hydrogen:

$$(4a) \qquad 2CO \rightleftarrows CO_2 + C$$

$$(6a) \qquad CO + H_2O \rightleftarrows CO_2 + H_2$$

Furthermore, Table 3 shows that the production of CO_2 is not influenced

Table 2. Carbon Deposition Equilibrium Constants

Temperature °C	Temperature °K	$Fe/FeO/Fe_3O_4$ $\frac{P_{H_2}}{P_{H_2O}}$ K_1	$\frac{P_{CO}}{P_{CO_2}}$ K_2	Carbon Oxidation $\frac{P_{CO} \times P_{CO}}{P_{CO_2}}$ K_4	$\frac{P_{H_2} \times P_{CO}}{P_{H_2O}}$ K_5	Water Shift $\frac{P_{H_2} \times P_{CO_2}}{P_{H_2O} \times P_{CO}}$ K_6
				µatm	µatm	
500		60.733	2.268	0.001620	0.2232	137.77
	250	42.523	2.123	0.01029	0.9291	90.26
550		29.391	1.974	0.07215	4.185	58.01
	300	22.039	1.861	0.3343	13.713	41.02
600		16.288	1.745	1.705	48.47	28.43
	350	12.898	1.652	6.200	132.1	21.31
650		10.065	1.556	24.71	387.1	15.67
	400	8.296	1.480	74.37	913.4	12.28
700		6.760	1.401	243.5	2,305	9.469
	450	5.751	1.339	629.8	4,849	7.698
750		4.851	1.270	1,760	10,846	6.162
	500	4.235	1.217	4,030	20,780	5.156
				atm	atm	
800		3.673	1.156	0.00931	0.04215	4.244
	550	3.276	1.114	0.02050	0.07479	3.648
850		3.005	1.022	0.04556	0.1399	3.071
	600	2.848	0.9416	0.08684	0.2329	2.682
900		2.687	0.8609	0.1759	0.4069	2.313
	650	2.564	0.8005	0.3124	0.6413	2.053
950		2.437	0.7393	0.5869	1.057	1.801
	700	2.239	0.7016	0.9698	1.591	1.641
1000		2.237	0.6453	1.731	2.498	1.443

by H_2 until the H_2 concentration becomes quite high. Therefore, the production of CO_2 at low H_2 concentrations can be attributed to reaction

$$(4a) \qquad 2CO \rightleftarrows CO_2 + C$$

and not to the reaction sequence

$$(5a) \quad CO + H_2 \rightleftarrows H_2O + C$$

$$(6a) \quad CO + H_2O \rightleftarrows CO_2 + H_2$$

Table 3. Effect of H_2 on Production of CO_2 at 550°C (6)

CO μatm	H_2 μatm	H_2O μatm	CO_2 μatm
10,000	40	4	45
10,000	1,800	35	45
10,000	3,200	80	57
10,000	5,800	200	94
9,750	11,000	820	270

Both water and carbon dioxide may oxidize iron, but water does so more readily in the temperature range in question. Thus, if iron is oxidized, water is more likely to be the oxidizing agent than carbon dioxide. Since increasing concentrations of hydrogen tend to inhibit carbon deposition and favor water production, it is probable that water plays a role in the decreased reactivity.

Iron oxide in the form FeO may exist at temperatures as low as 560°C (17). Therefore, the possibility of the following reaction

exists at metal dusting temperatures:

$$(1a) \quad Fe + H_2O \rightleftarrows FeO + H_2$$

Assuming that Fe metal is the catalyst, reaction (1a) also tends to decrease catalytic surface and, hence, decrease reactivity.

In summary, for iron in hydrogen-carbon monoxide atmospheres it appears that increasing hydrogen concentration favors water production which, in turn, favors reduction of catalytic surface area by oxidation of the iron. The hydrogen is no longer capable of regeneration of the Fe metal and reactivity decreases.

Figure 6 shows the variation of reactivity with temperature for pure cobalt in atmospheres containing hydrogen. The reactivity of cobalt was similar to iron, suggesting that similar mechanisms prevailed. It has been shown that carbon formation on cobalt, as on iron, involves a carbide intermediate (9,12). The presence of hydrogen definitely increased reactivity, while an increase in hydrogen content from 5% to 10% in CO appeared to retard the reaction. As with iron, increasing temperature favored decreasing reactivity.

The reactivity of nickel 200 is shown in Figure 7. Results were consistent with those of earlier researchers (29) who found that nickel-base alloys show increasing reactivity with increasing temperature. Reactivity also increased with increasing hydrogen content. A reactivity peak was noted at about 625°C for a 5% H_2-CO mixture. Former researchers (29) found a peak at about 775°C for a 1.92% H_2-CO mixture. Insufficient data were available to confirm a low temperature peak for the 10% H_2-CO atmosphere.

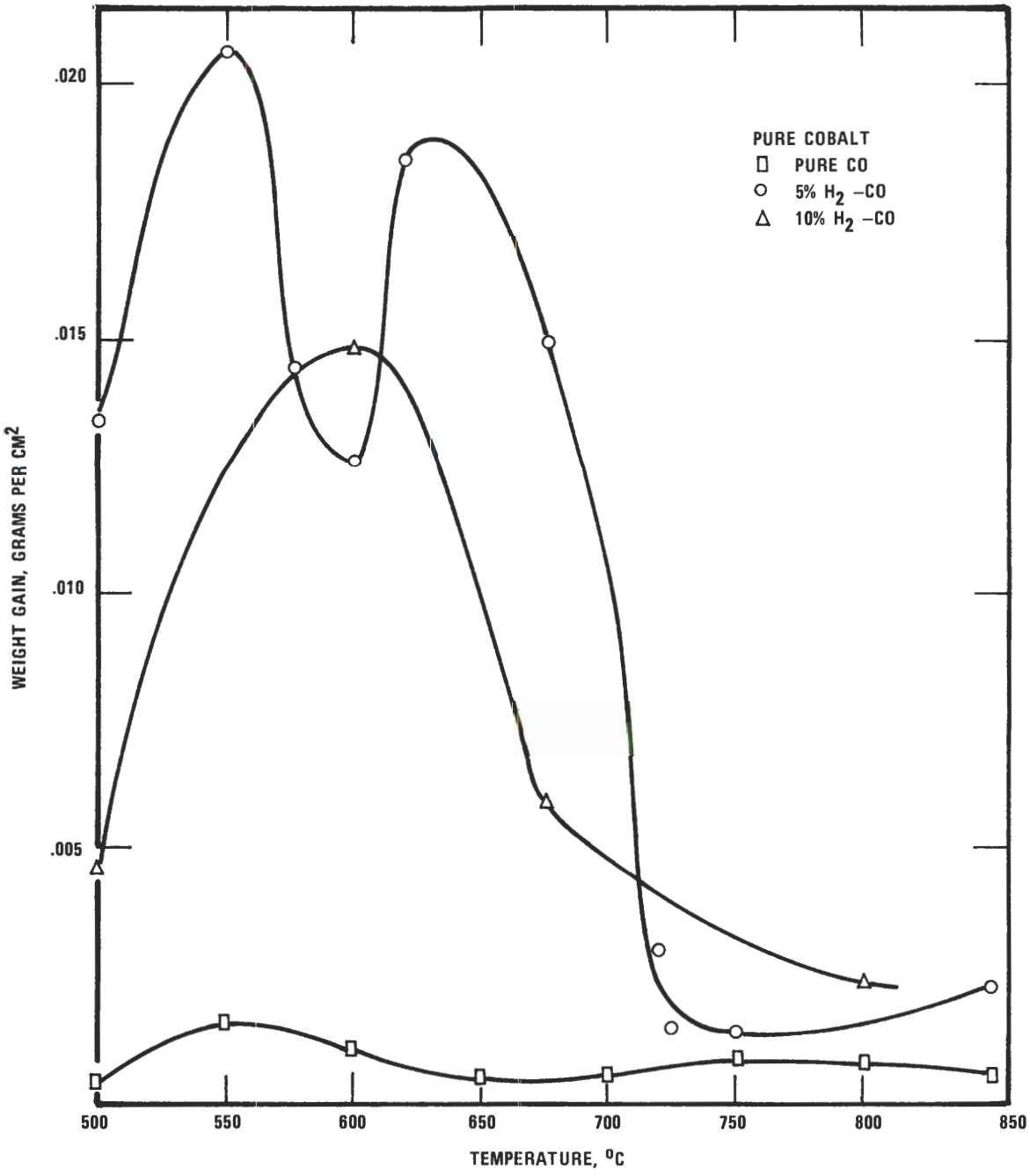

Figure 6. The Reactivity of Pure Cobalt in Pure CO, 5% H_2-CO, and 10% H_2-CO Environments.

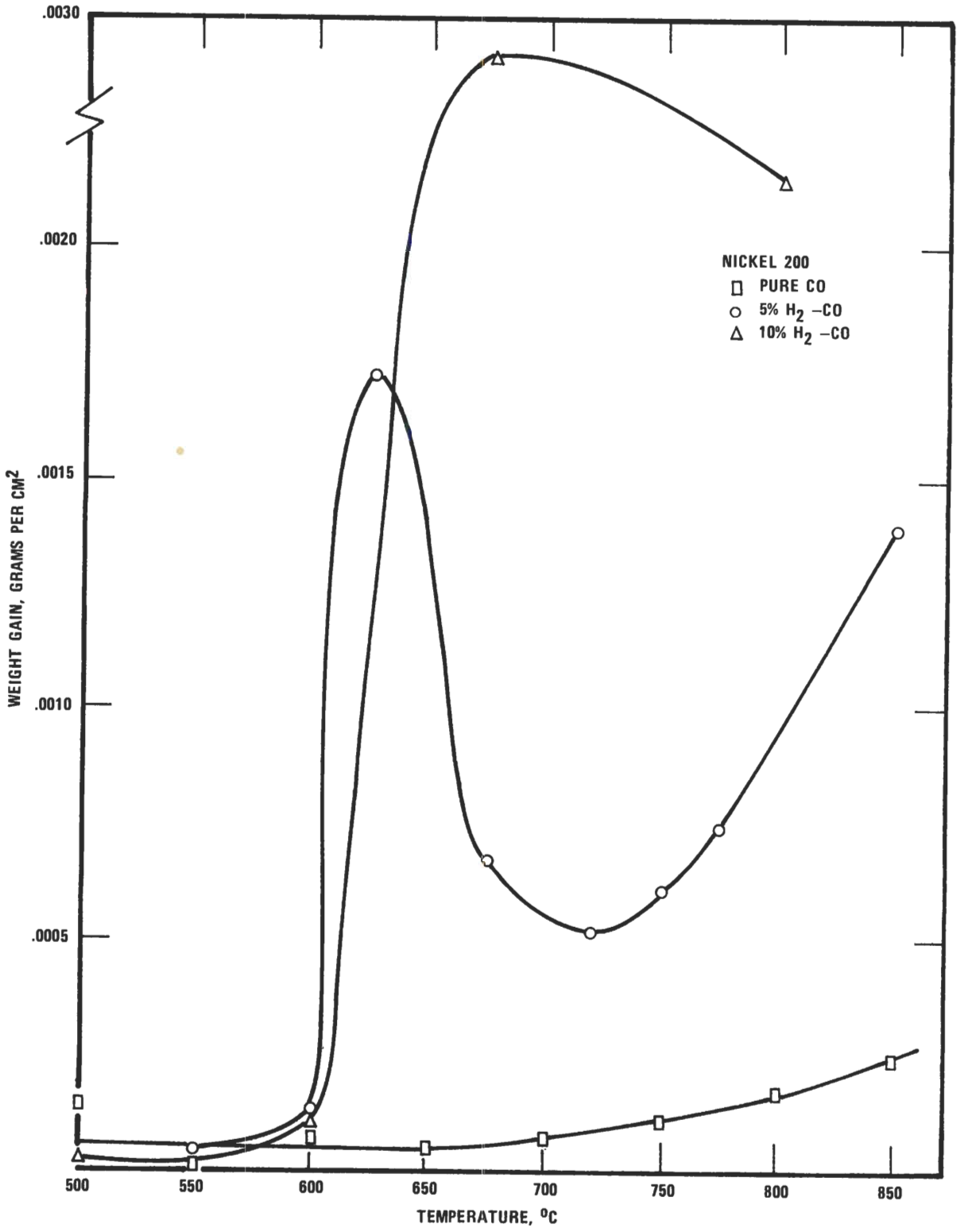

Figure 7. The Reactivity of Nickel 200 in Pure CO, 5% H_2-CO, and 10% H_2-CO Environments.

Figures 8 and 9 show the behavior of types 302 and 316 stainless steels, respectively, in H_2-CO environments. In general, the iron-base alloys reacted similarly to iron, but the nickel present in the 300 series shifted the reactivity maxima to a higher temperature than the temperature of maximum reactivity for iron. Both types of stainless steels exhibited reactivity peaks at about 650°C for pure CO and 5% H_2-CO atmospheres. Increasing the hydrogen content to 10% H_2 in CO substantially reduced reactivity. Type 316 was slightly more reactive than type 302 in pure CO at 650°C. The presence of 2-3% molybdenum in type 316 resulting in the formation of molybdenum carbides was probably responsible for this variation in reactivity.

The reactivity of type 416 stainless steel is shown in Figure 10. Significant reactivity was found only in the temperature range 550-600°C, and a reaction peak was found at 550°C. The low temperature reactivity was attributed to the absence of nickel in type 416 stainless. Nickel was found to promote high temperature reactivity and all materials containing nickel showed low reactivities in the temperature range where type 416 showed maximum reactivity.

Reactivity characteristics of Inconel 600 are shown in Figure 11. Maximum reactivity was found at 750°C for pure CO and in the range 675°C to 775°C for the 5% H_2-CO mixture. Insufficient data were available for significant conclusions for the 10% H_2-CO mixtures, but reactivities tended to be lower than for the 5% H_2-CO atmosphere. As expected, Inconel 600 (75% nickel) exhibited reactivity similar to nickel 200.

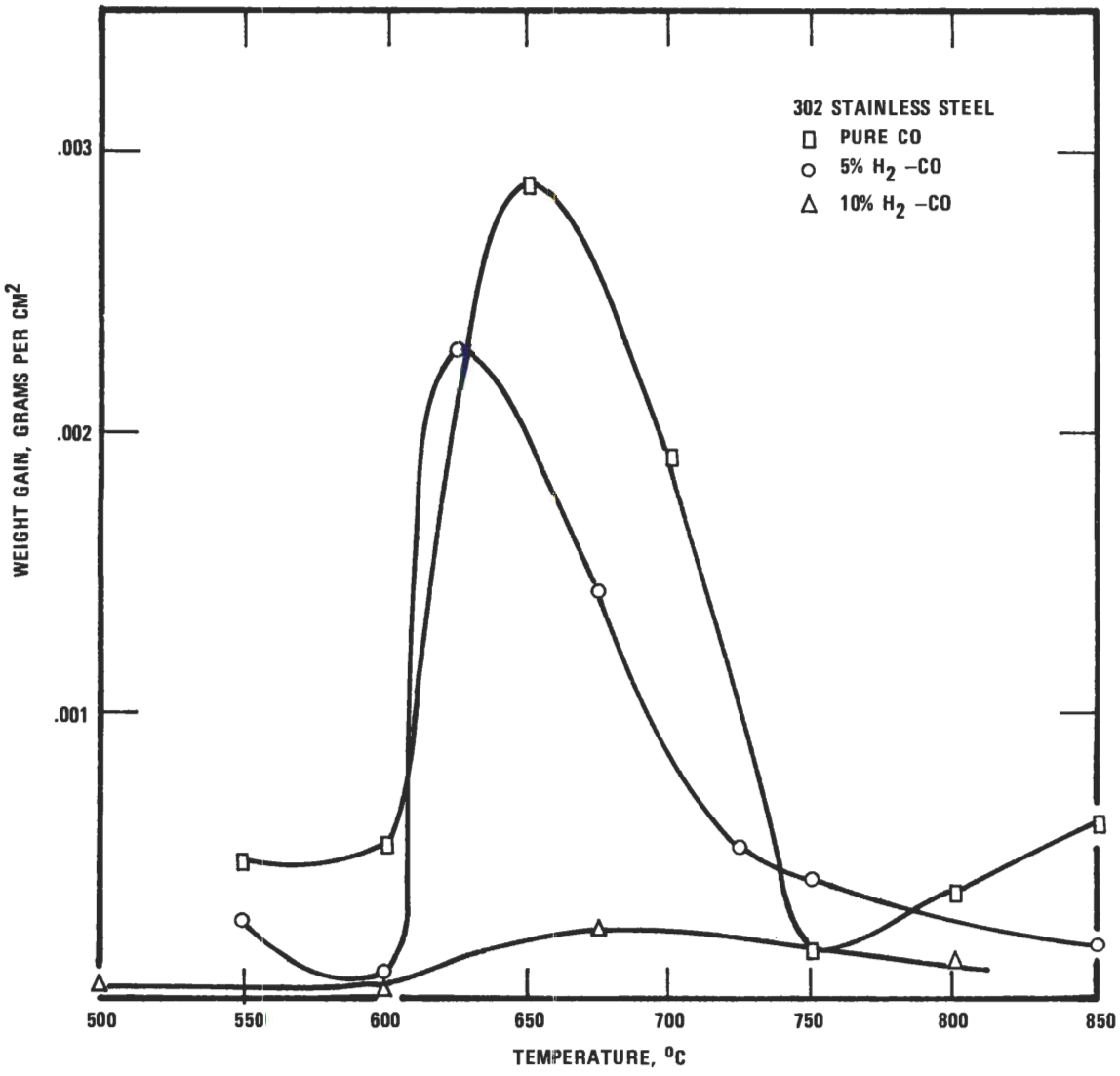

Figure 8. The Reactivity of 302 Stainless Steel in Pure CO, 5% H_2-CO, and 10% H_2-CO Environments.

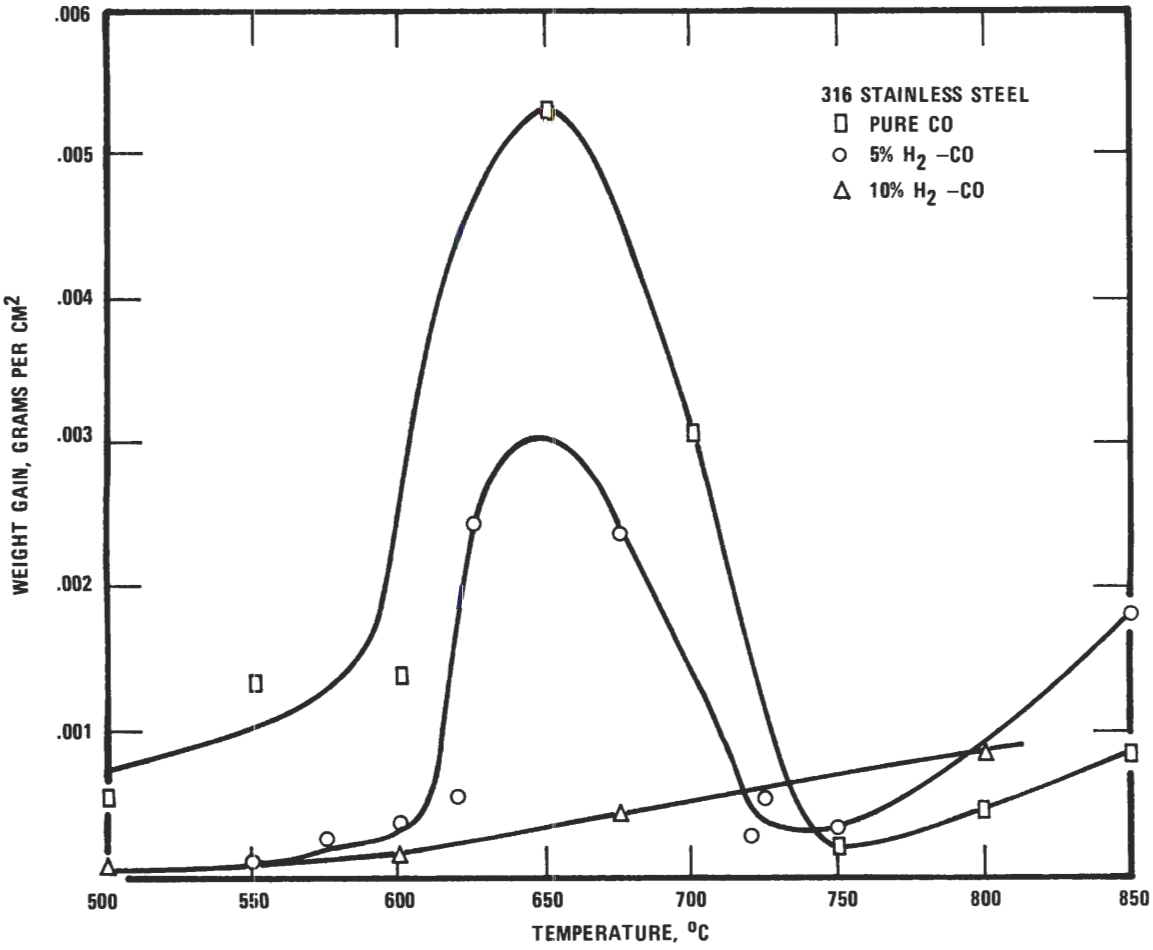

Figure 9. The Reactivity of 316 Stainless Steel in Pure CO, 5% H_2-CO, and 10% H_2-CO Environments.

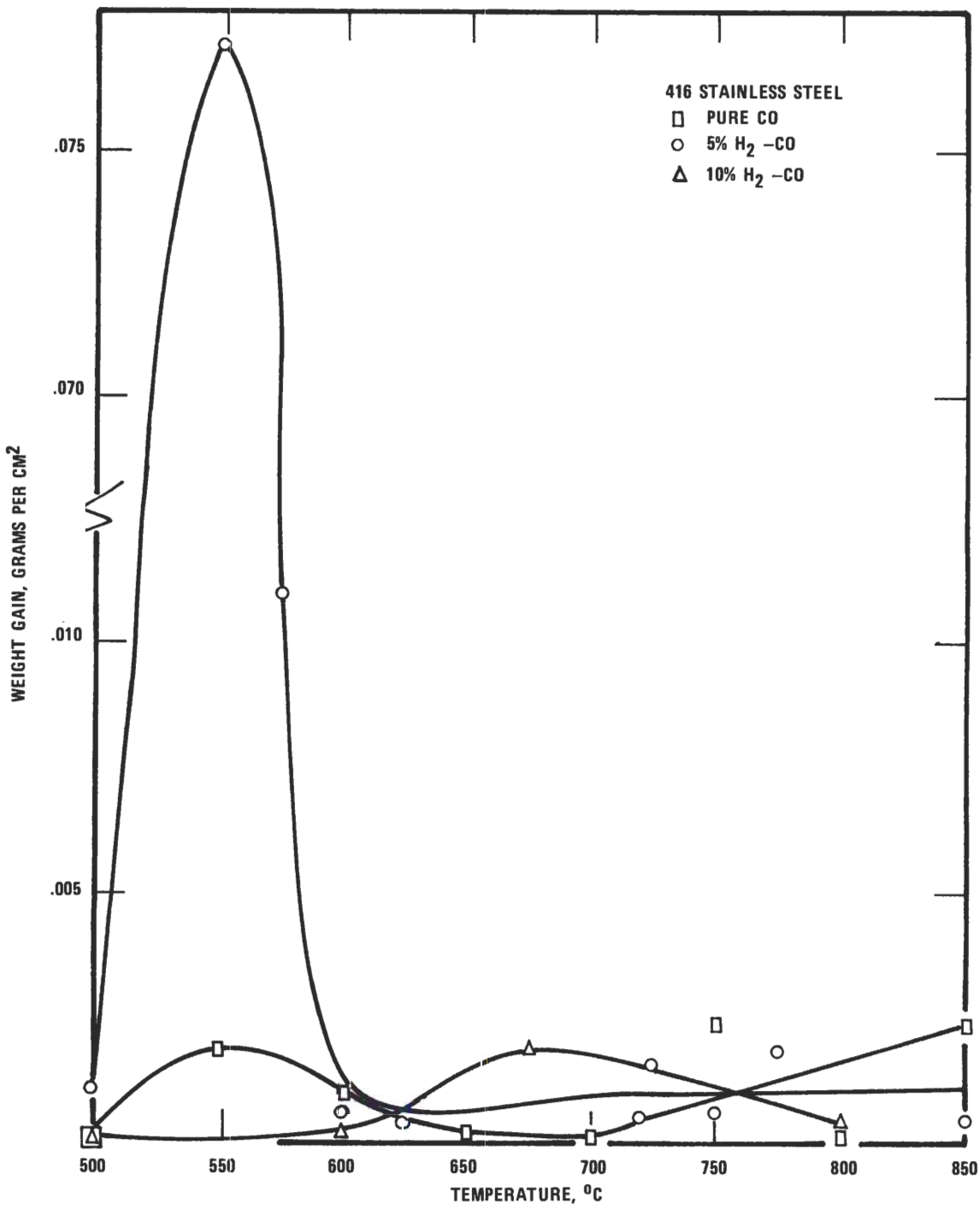

Figure 10. The Reactivity of 416 Stainless Steel in Pure CO, 5% H_2-CO, and 10% H_2-CO Environments.

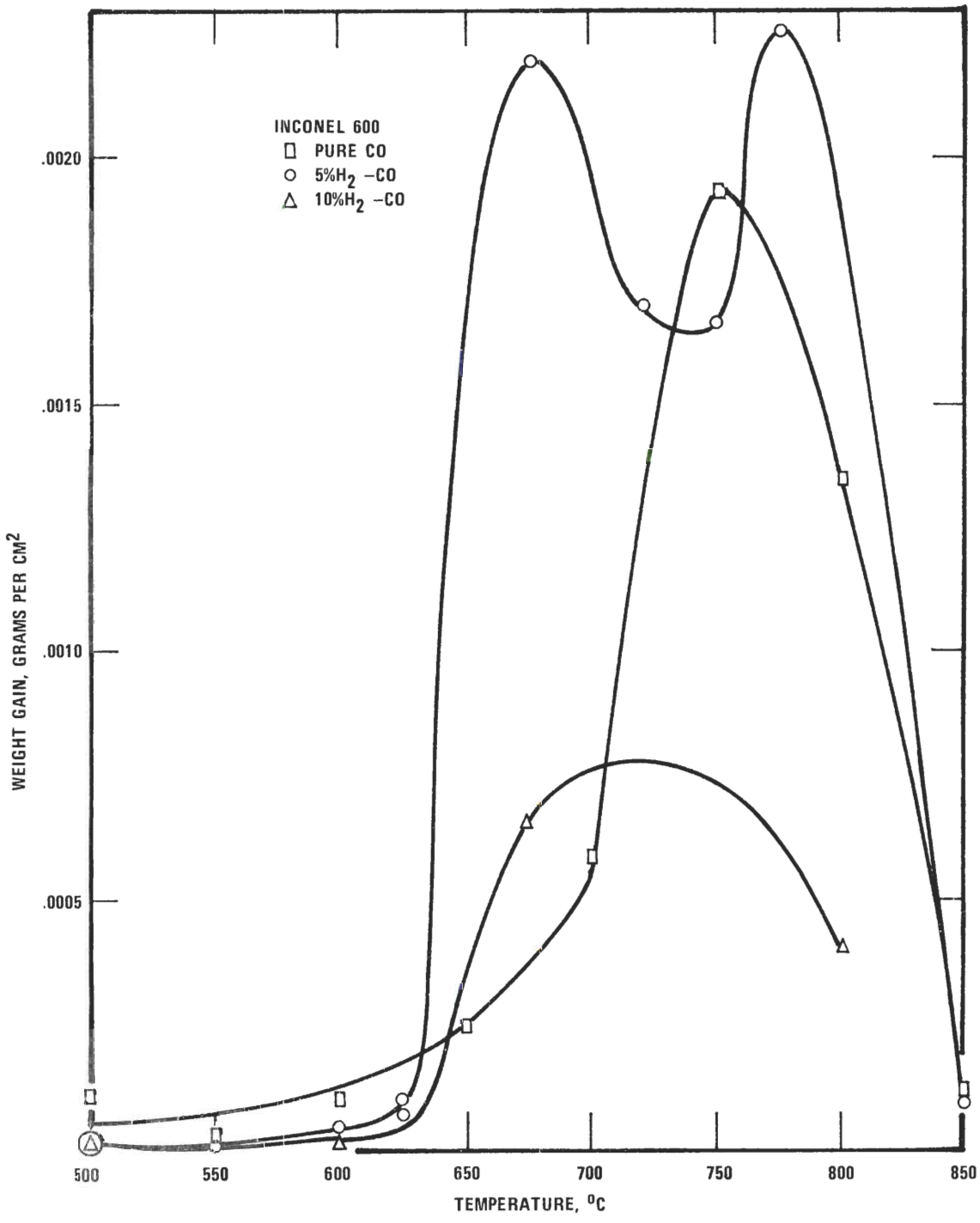

Figure 11. The Reactivity of Inconel 600 in Pure CO, 5% H_2-CO, and 10% H_2-CO Environments.

Surface Reaction Products

Scanning electron micrographs (SEM) of surface reaction products revealed information about the structure of the carbonaceous deposits. Iron and cobalt, shown in Figures 12 and 13, respectively, exhibited characteristically bulky, porous products compared to the other materials. The similarity of the micrographs of iron and cobalt suggests that very similar reaction mechanisms prevailed during the formation of the surface product. It has been shown, for example, that the decomposition of CO on both metals proceeds through the formation of an intermediate carbide (9).

Deposits on nickel 200 (Figure 14) and Inconel 600 (Figure 15) were generally smaller and of more uniform particle size than those on the iron-base alloys. The 300 series stainless steels, shown in Figures 16 and 17, were characterized by filamentary carbon deposits. Reaction products on type 316 stainless were a combination of flakes and filaments, whereas type 302 exhibited filaments almost exclusively. Type 416 stainless (Figure 18) formed a reaction product of roughly spherical particles of uniform size and low porosity.

Electron diffraction studies of surface deposits on iron reacted at 600°C in 10% H_2-CO confirmed the presence of graphite and Fe_3C, but failed to detect oxides. It is likely that oxides were formed and reduced by the hydrogen, since hydrogen is used commercially to reduce oxides in catalyst preparation.

Optical Microscopy

Several samples were examined to determine the microstructure of the wires after exposure to the carbon monoxide-hydrogen atmospheres. The purpose of this investigation was to establish the relationship

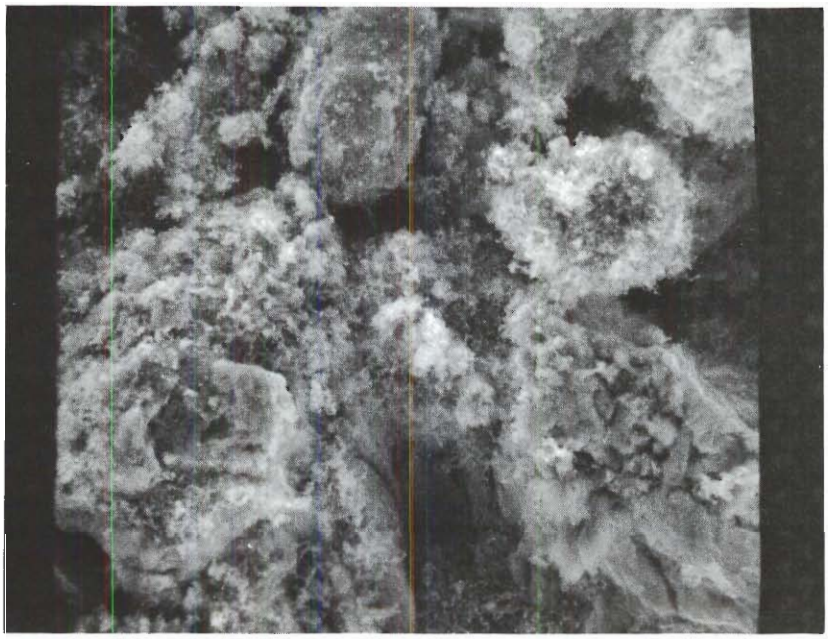

Figure 12. Electron Micrograph of Surface Reaction Products on Pure Iron Reacted at 625°C in 5% H_2-CO for 20 Hours. Sample No. 44 SEM 1780X

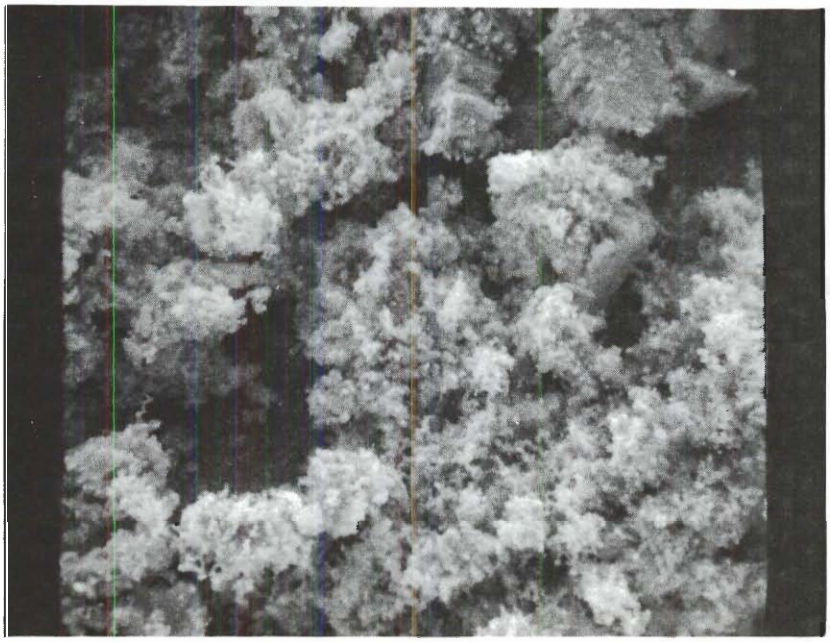

Figure 13. Electron Micrograph of Surface Reaction Products on Pure Cobalt Reacted at 625°C in 5% H_2-CO for 20 Hours. Sample No. 8 SEM 1780X

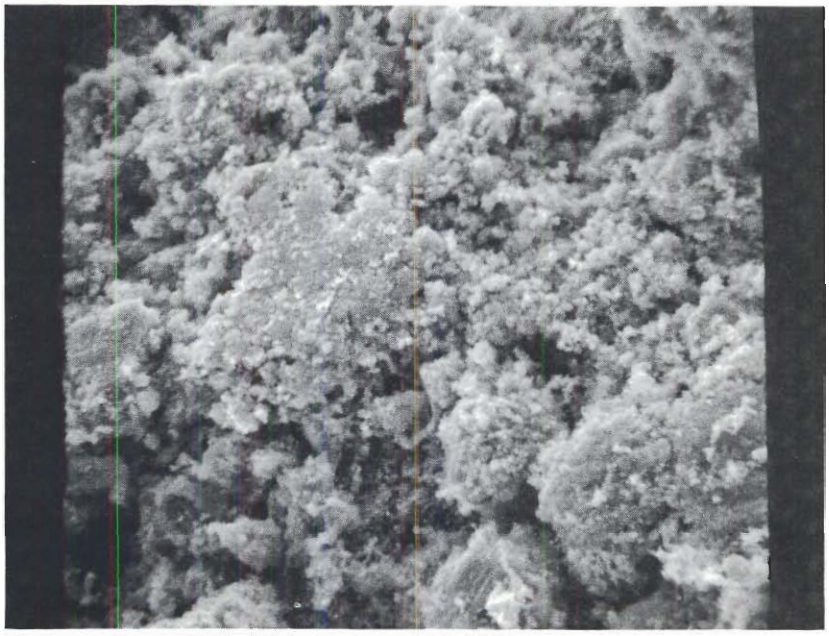

Figure 14. Electron Micrograph of Surface Reaction Products on Nickel 200 Reacted at 675°C in 10% H_2-CO for 20 Hours.
Sample No. 33 SEM 1780X

Figure 15. Electron Micrograph of Surface Reaction Products on Inconel 600 Reacted at 775°C in 5% H_2-CO for 20 Hours.
Sample No. 118 SEM 1780X

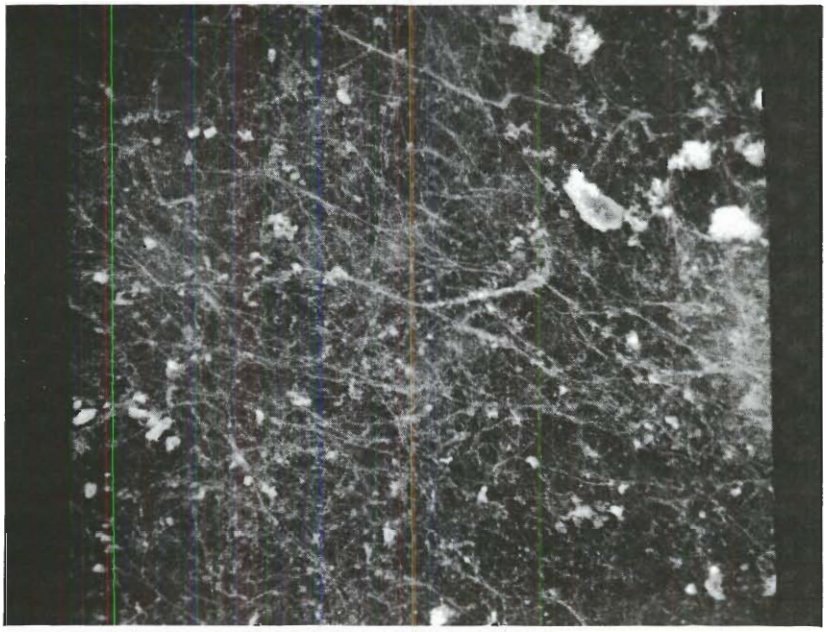

Figure 16a. Electron Micrograph of Surface Reaction Products on 302 Stainless Steel Reacted at 625°C in 5% H_2-CO for 20 Hours. Sample No. 14 SEM 1780X

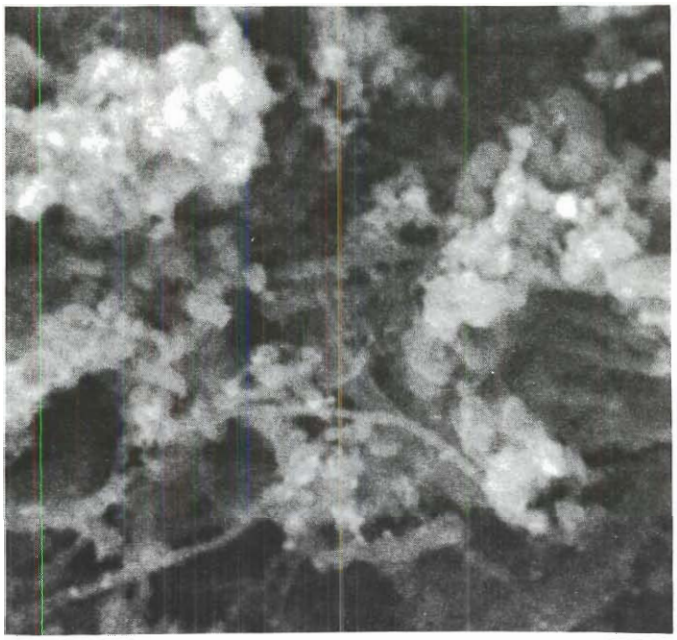

Figure 16b. Electron Micrograph of Surface Reaction Products on 302 Stainless Steel Reacted at 625°C in 5% H_2-CO for 20 Hours. Sample No. 14 SEM 8900X

Figure 17. Electron Micrograph of Surface Reaction Products on 316 Stainless Steel Reacted at 650°C in Pure CO for 20 Hours. Sample No. 176 SEM 1780X

Figure 18. Electron Micrograph of Surface Reaction Products on 416 Stainless Steel Reacted at 550°C in 5% H_2-CO for 20 Hours. Sample No. 19 SEM 1780X

between the microstructure and the reactivity. The samples selected for examination exhibited either exceptionally high or low reactivities under particular experimental conditions.

Figures 19a and b show the microstructure of iron after exposure to 5% H_2-CO at 625°C for 20 hours. The 5% H_2-CO atmosphere was found to promote maximum reactivity for iron. Figure 20 shows the structure of iron reacted in pure CO at 600°C for 20 hours. The ferrite grains of the sample reacted in the 5% H_2-CO mixture are considerably smaller than the grains of the sample reacted in pure CO. In addition, hydrogen appears to promote surface attack and graphitization. The periphery of the sample in Figure 19a shows extensive deterioration and carbon deposition, whereas the sample in Figure 20 exhibits a moderate, uniform surface attack. This phenomenon may be attributed to the ability of hydrogen to convert the iron carbides to elemental iron, thereby exposing fresh catalytic surface for the decomposition of carbon monoxide. Since the decomposition occurs at the gas-metal interface, it is expected that the metal surface should experience severe attack.

Figures 21 and 22 show the microstructure of samples of 302 stainless steel reacted in 5% H_2-CO at 625°C and 10% H_2-CO at 600°C, respectively. Carbides, particularly in the grain boundaries, are prevalent in both samples. The sample reacted in 10% H_2-CO exhibited considerably less weight gain than the sample reacted in 5% H_2-CO. Since the amounts of internal carburization appear similar, it is likely that the difference in reactivities is attributable to variation in amounts of surface deposition. Visual observation and gravimetric determinations confirmed this conclusion.

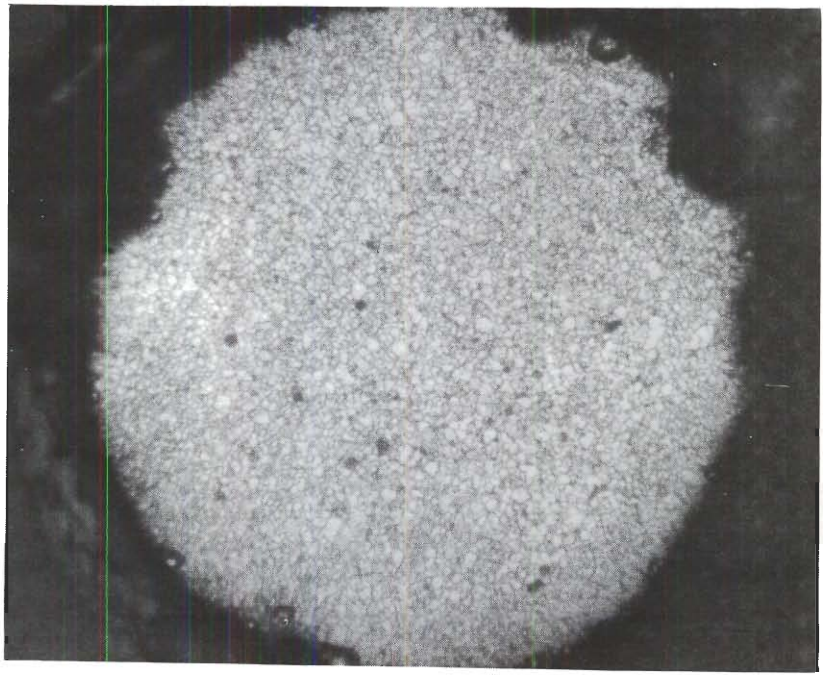

Figure 19a. The Microstructure of Pure Iron Reacted at 625°C in 5% H_2-CO for 20 Hours. (Nital) Sample No. 44 160X

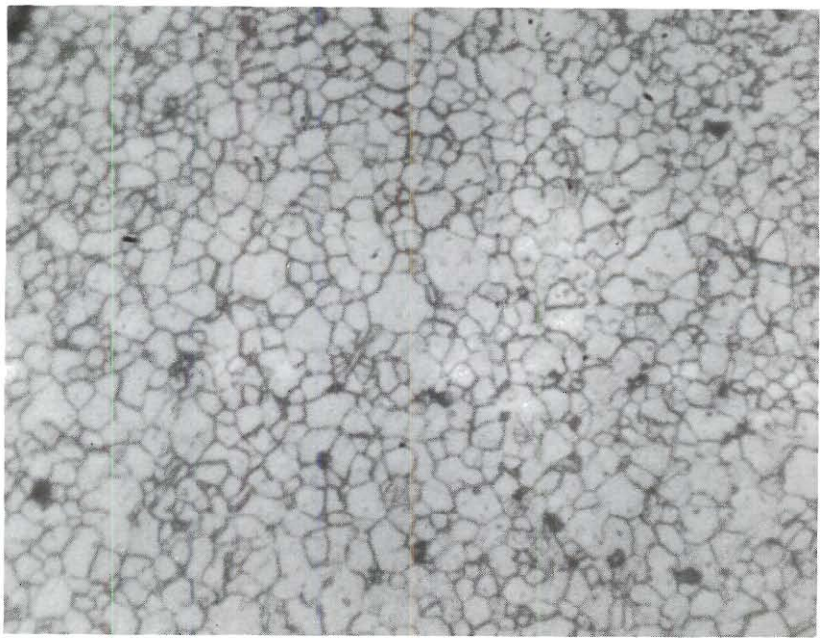

Figure 19b. The Microstructure of Pure Iron Reacted at 625°C in 5% H_2-CO for 20 Hours. (Nital) Sample No. 44 600X

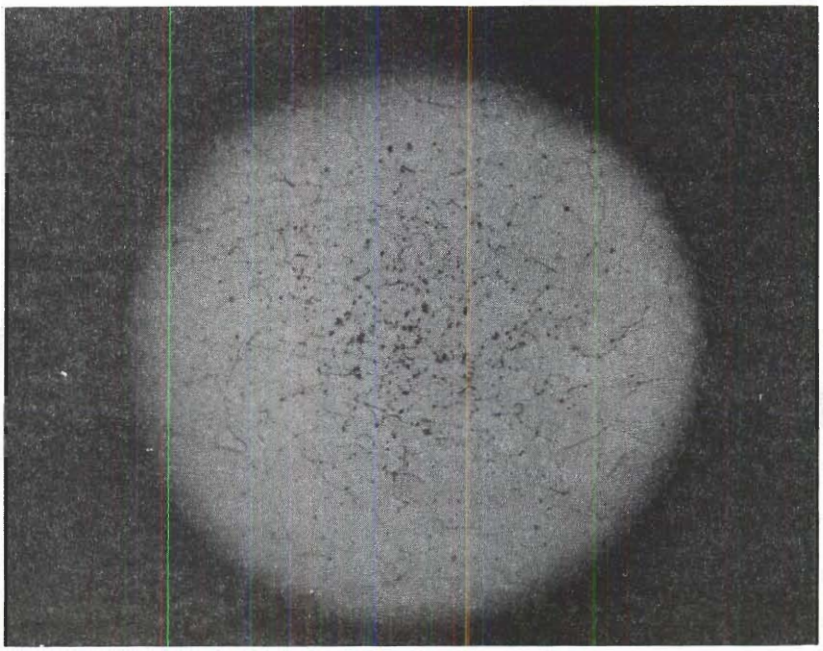

Figure 20. The Microstructure of Pure Iron Reacted at 600°C in Pure CO for 20 Hours. (Nital) Sample No. 122 150X

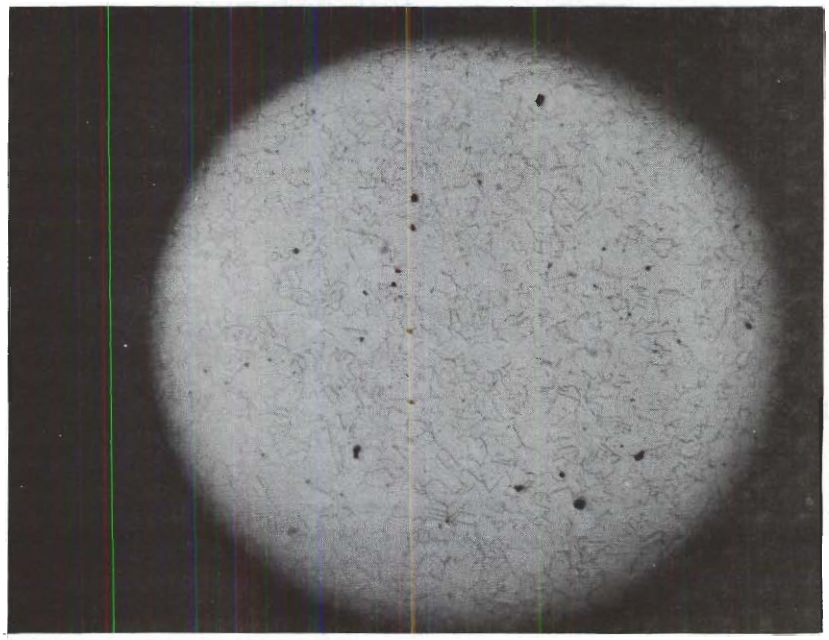

Figure 21a. The Microstructure of 302 Stainless Steel Reacted at 625°C in 5% H_2-CO for 20 Hours. (Glyceregia) Sample No. 14 150X

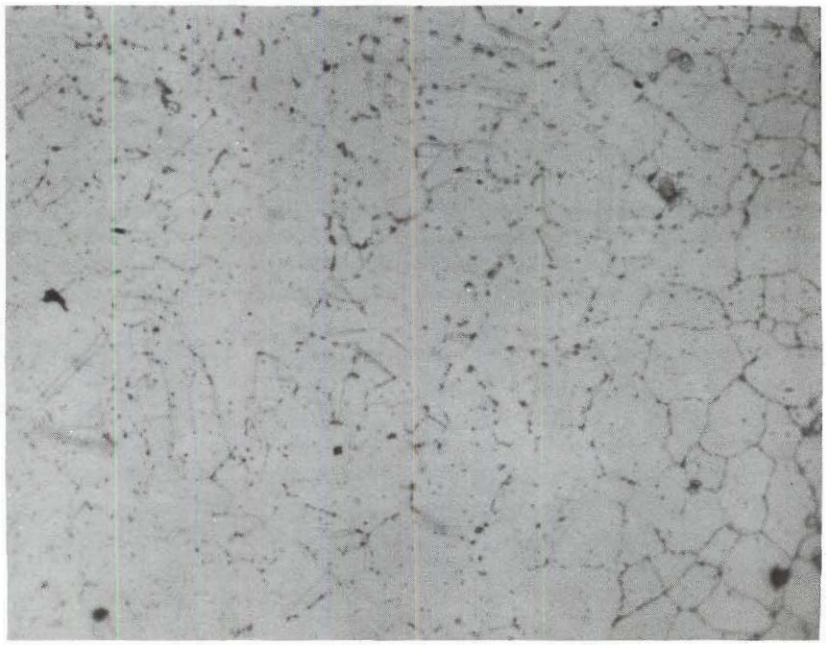

Figure 21b. The Microstructure of 302 Stainless Steel Reacted at 625°C in 5% H_2-CO for 20 Hours. (Glyceregia) Sample No. 14 500X

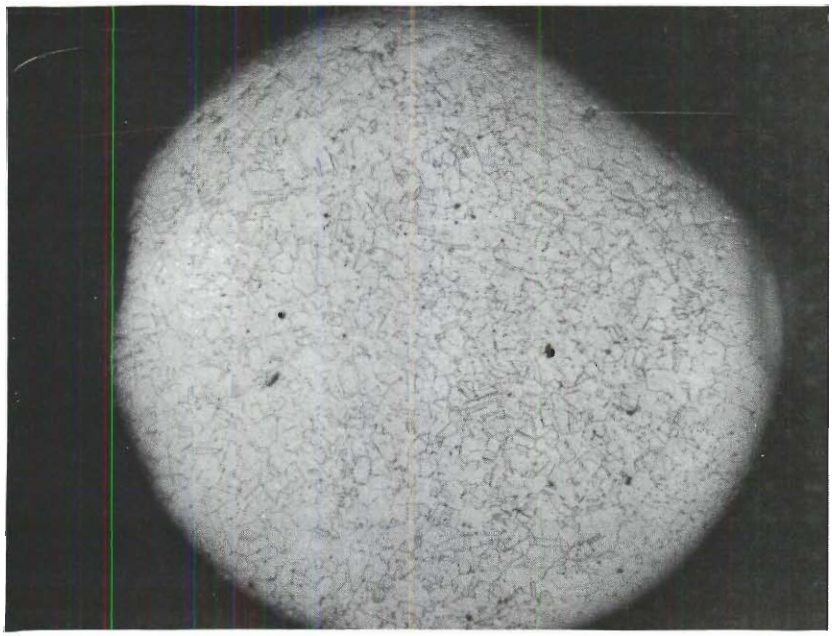

Figure 22a. The Microstructure of 302 Stainless Steel Reacted at 600°C in 10% H_2-CO for 20 Hours. (Glyceregia) Sample No. 63 130X

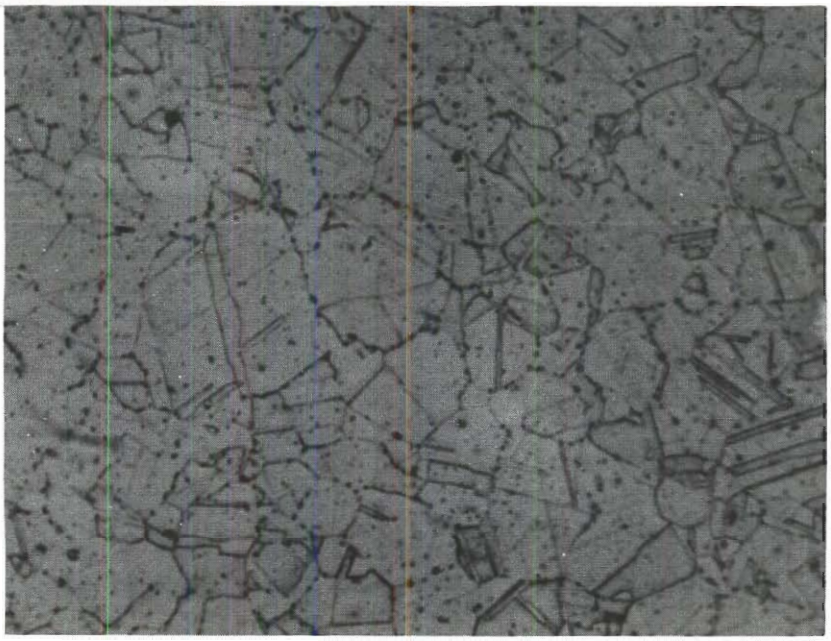

Figure 22b. The Microstructure of 302 Stainless Steel Reacted at 600°C in 10% H_2-CO for 20 Hours. (Glyceregia) Sample No. 63 600X

Methane-Hydrogen Mixtures

Reactivity Studies

The reactivity characteristics of pure iron in pure methane and a 5% H_2-CH_4 mixture are shown in Figure 23. Significant differences between the two atmospheres were not evident, but the addition of hydrogen tended to retard the reaction in the temperature range of 600° to 750° and accelerate reactivity above 800°C. These results can be best seen by considering the differences in slopes of the straight portions of the curves for iron in Figure 23.

Figure 24 shows the reactivity of pure cobalt in CH_4 and 5% H_2-CH_4 environments. Both atmospheres promoted increasing reactivity with increasing temperature. The reactivity in the 5% H_2-CH_4 atmosphere was generally greater than in pure methane above 800°C, but no significant reaction peaks were noted for either environment.

Nickel 200 in pure methane showed a reaction maximum at 800°C. Reactivity then decreased with increasing temperature. Figure 25 shows that in the 5% H_2-CH_4 atmosphere a reaction peak occurred at 700°C followed by a decline in reactivity up to 750°C where reactivity began to increase to a maximum at 900°C. It should be noted that hydrogen also promoted significant reactivity on nickel 200 in carbon monoxide atmospheres at about 700°C. Thus, the adsorption of hydrogen probably becomes important in the temperature range 650° to 750°C (36).

Figures 26 and 27 show the reactivities of 302 and 316 stainless steels, respectively, in CH_4 and 5% H_2-CH_4 atmospheres. Curves for

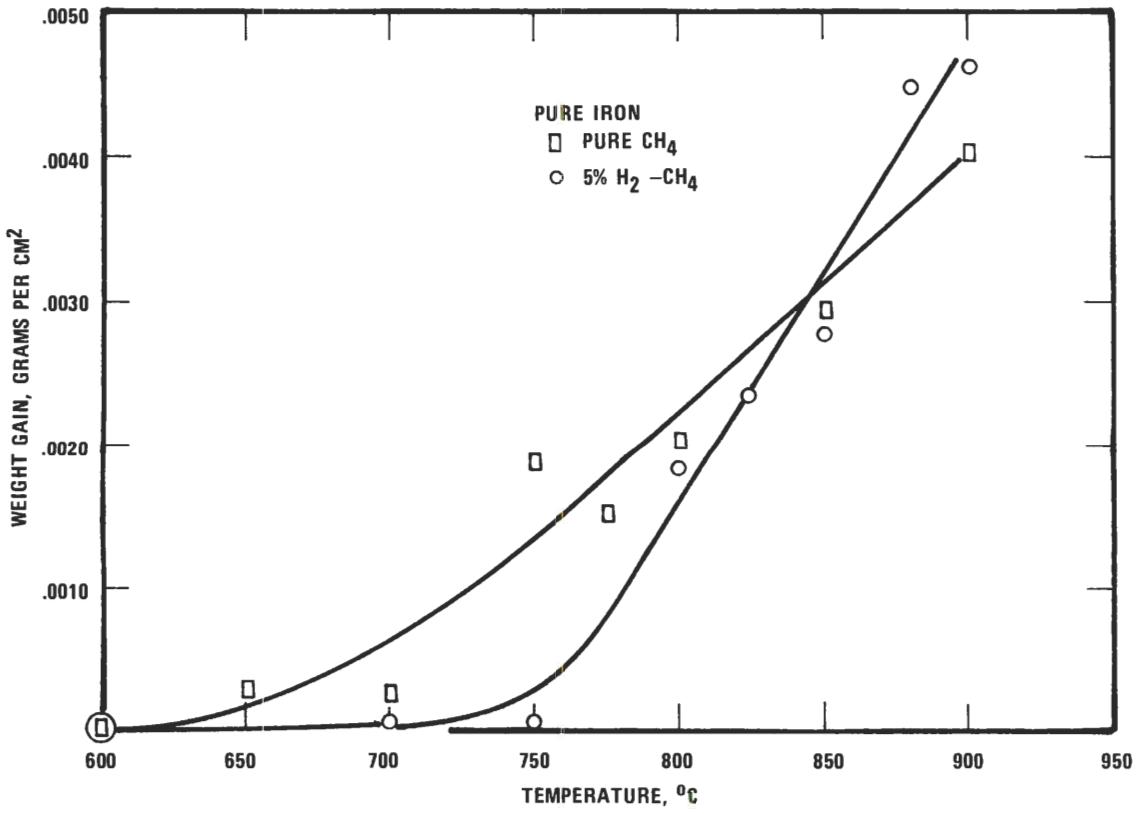

Figure 23. The Reactivity of Pure Iron in Pure CH_4 and 5% H_2-CH_4 Environments.

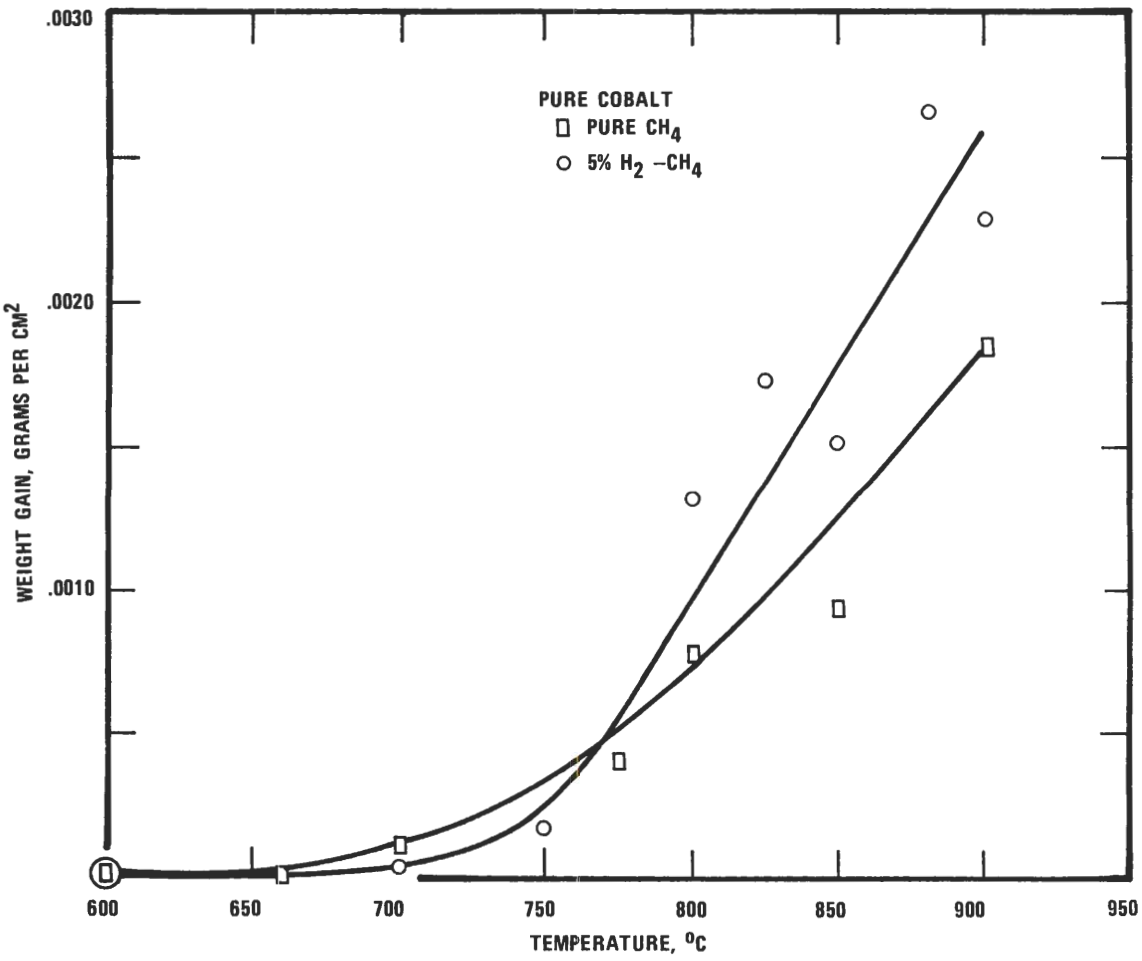

Figure 24. The Reactivity of Pure Cobalt in Pure CH_4 and 5% H_2-CH_4 Environments.

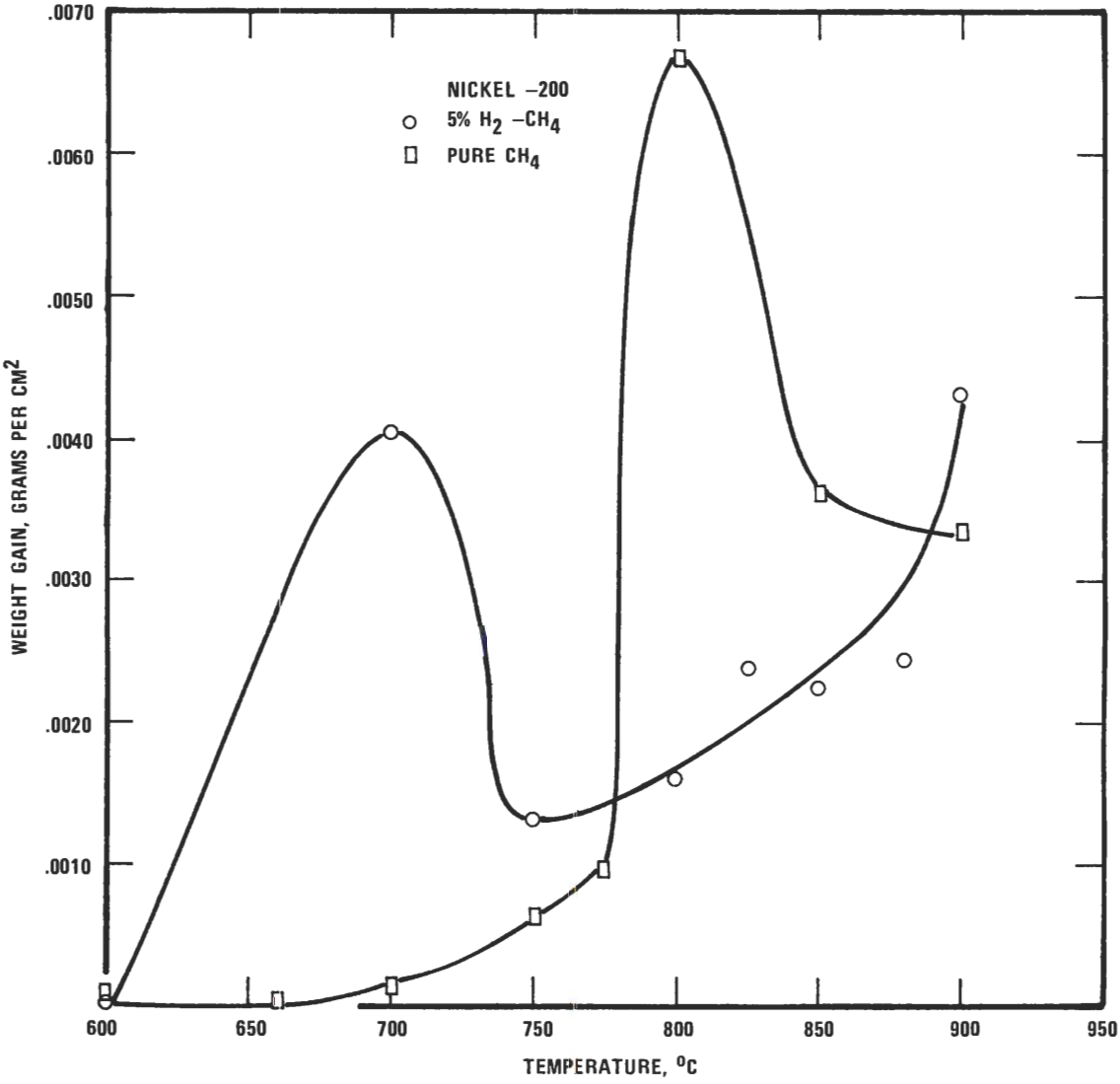

Figure 25. The Reactivity of Nickel 200 in 5% H_2-CH_4 and Pure CH_4 Environments.

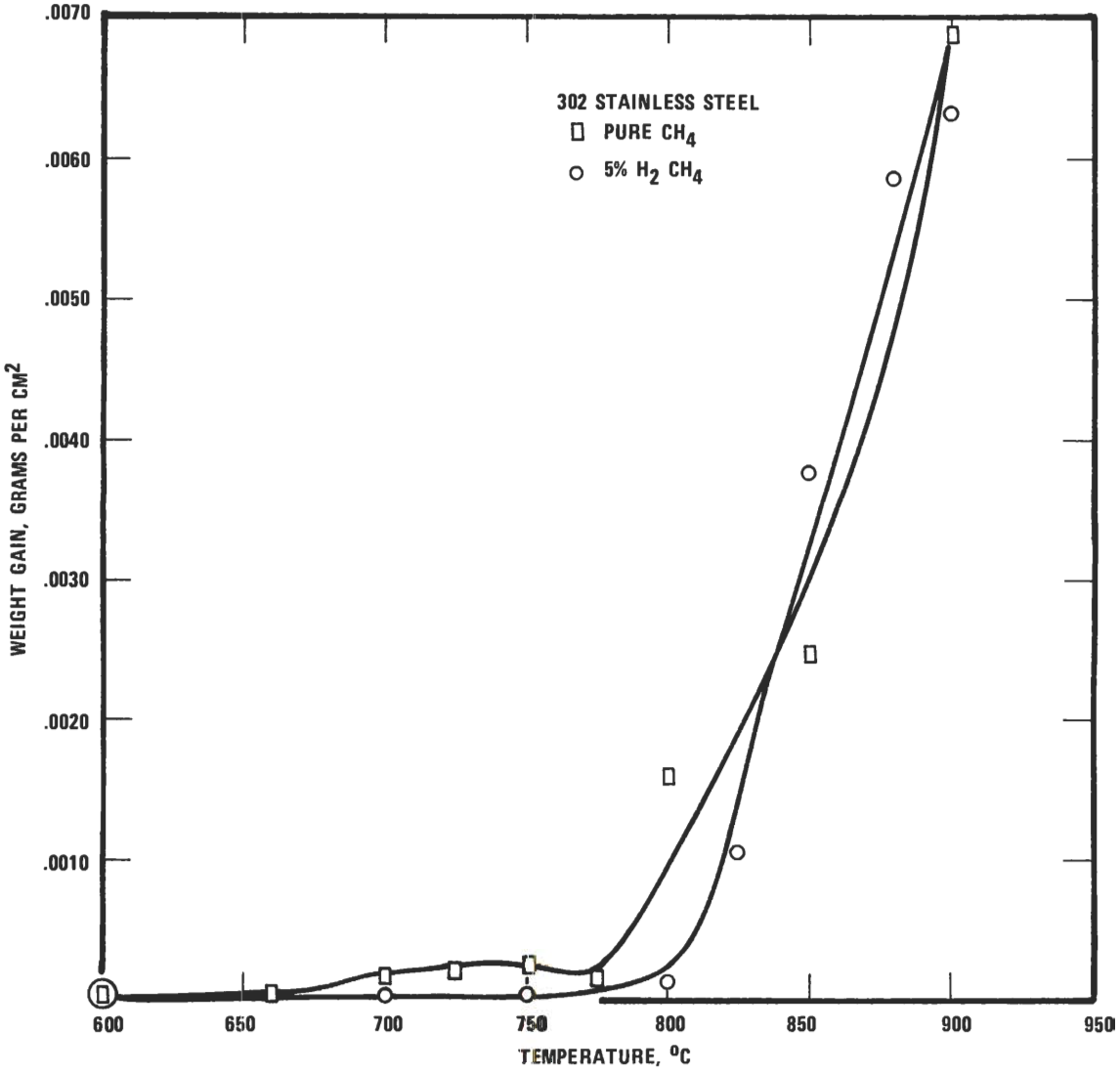

Figure 26. The Reactivity of 302 Stainless Steel in Pure CH_4 and 5% H_2-CH_4 Environments.

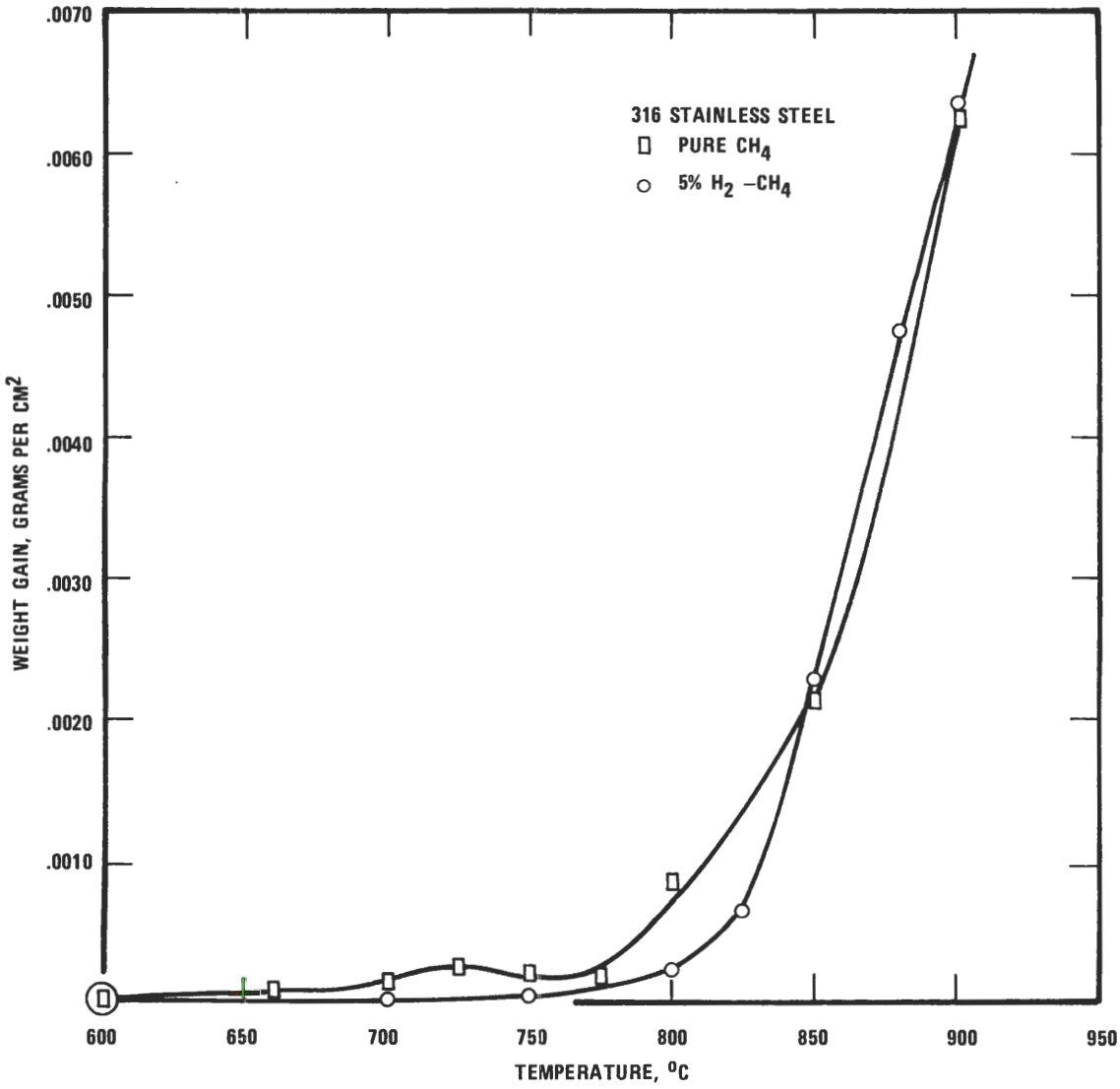

Figure 27. The Reactivity of 316 Stainless Steel in Pure CH_4 and 5% H_2-CH_4 Environments.

both 302 and 316 were essentially identical, indicating that the slight differences in nickel, chromium, and molybdenum contents between 302 and 316 did not markedly affect the reactivity. The only notable difference between the reactivities in pure methane and the hydrogen-methane mixture occurred in the temperature range 750° to 850° where samples reacted in the 5% H_2-CH_4 mixture showed less reactivity than those in the pure CH_4 environments.

Type 416 stainless steel, shown in Figure 28, exhibited good dusting resistance. In the range 675° to 775°C more reactivity was noted for pure methane than for the 5% H_2-CH_4 mixture. Above 800°C the curves nearly coincided with reactivities increasing with increasing temperature.

Reactivity characteristics of Inconel 600 are given in Figure 29. Practically no difference was noted between the pure and mixed atmospheres except for a higher reaction peak at 775°C in pure CH_4. Abrupt increases in reactivity were found above 850°C with maximum reactivity at 900°C.

In general, the materials tested showed similar reactivities in both pure CH_4 and H_2-CH_4 mixtures. This result suggests that hydrogen plays a minor role in the reaction mechanism in hydrocarbon environments. The endothermic thermal decomposition of methane to carbon and hydrogen occurs between 650° and 980°C and 10 to 30 psig (36,37). Since chromium, molybdenum, titanium, nickel, iron, and cobalt are found to catalytically promote maximum hydrogen production, it is unlikely that small amounts of hydrogen initially in the system should significantly affect the reaction characteristics.

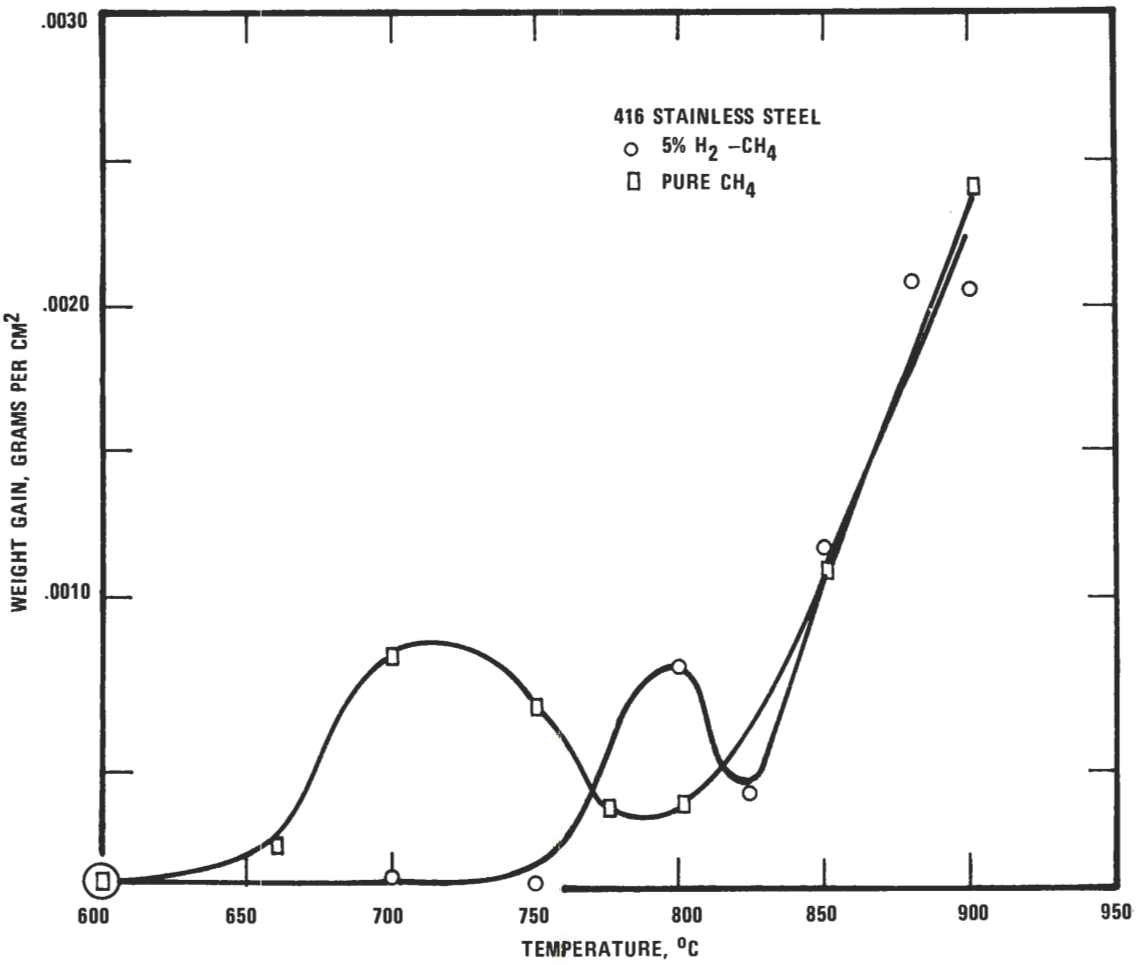

Figure 28. The Reactivity of 416 Stainless Steel in 5% H_2-CH_4 and Pure CH_4 Environments.

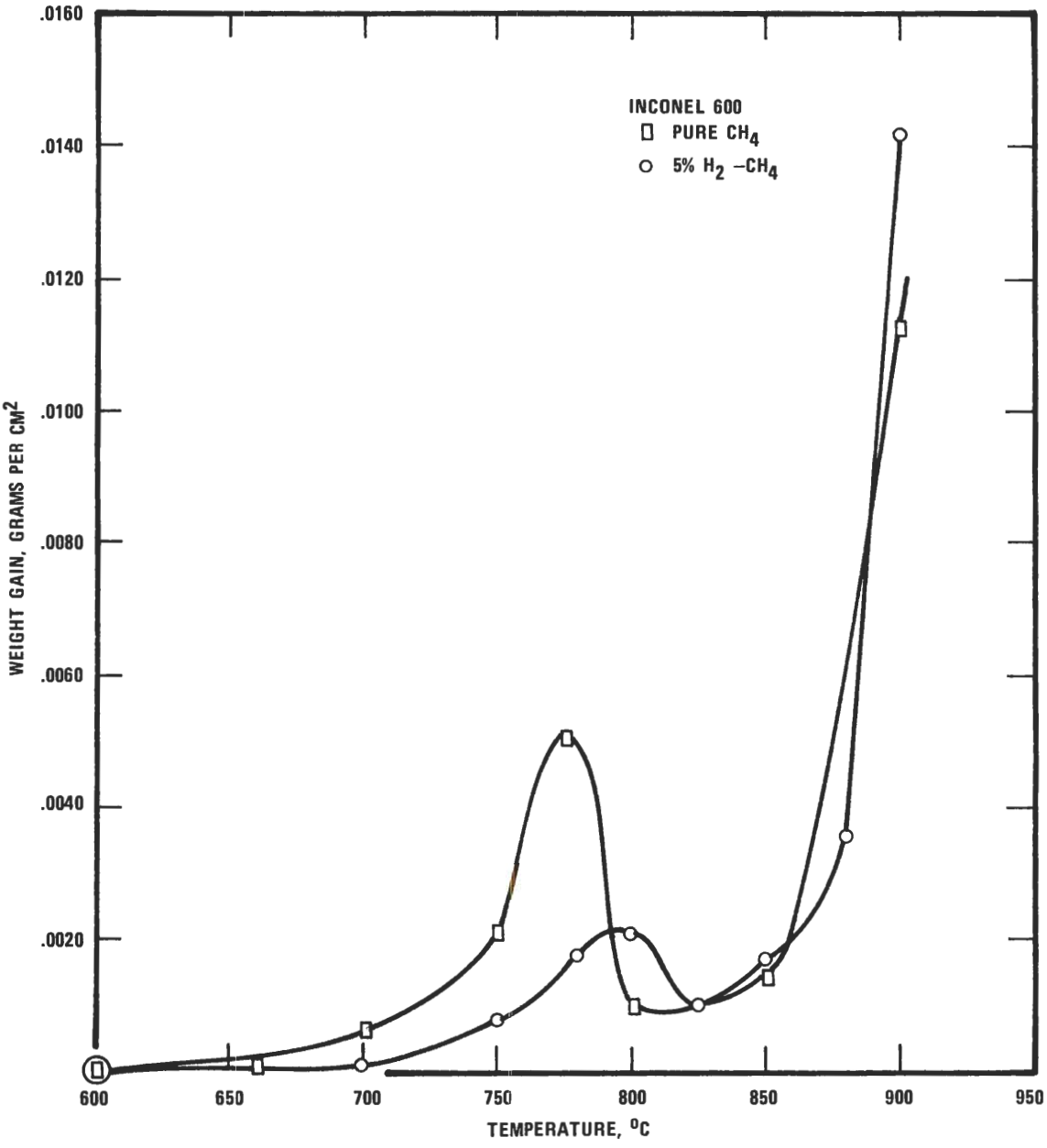

Figure 29. The Reactivity of Inconel 600 in Pure CH_4 and 5% H_2-CH_4 Environments.

Surface Reaction Products

Small structural differences in surface deposits were noted for samples reacted in methane-hydrogen atmospheres and examined with the scanning electron microscope (SEM). Iron, 302 stainless, and 316 stainless, shown in Figures 30, 31, and 32, respectively, exhibited spherical deposits of roughly the same particle size. Cobalt (Figure 33) formed a porous product composed of aggregates of particles slightly larger than those of the iron-base materials. Nickel 200, shown in Figure 34, produced a bulky, fluffy reaction product. Deposits on Inconel 600 (Figure 35) were extremely porous and slightly smaller than those on the other materials, and surface products on 416 stainless (Figure 36) were characterized by agglomerations of spherical particles interspersed with rod-like platelets.

The basic similarity of the surface reaction products on the materials reacted in the H_2-CH_4 atmospheres suggests that the chemical compositions of the samples had little effect on the reaction products formed. All of the materials tested have been shown to promote the decomposition of methane above 650°C (36,37) and it was found in this study that significant reaction occurred only at temperatures above 650°C. Furthermore, the ability of methane to polymerize has been established in the laboratory (38) and confirmed by mass spectroscopy (39). Thus, the surface products are probably combinations of carbon and hydrocarbons of various chain lengths. Precise identification of the reaction products was beyond the scope of this work.

Figure 30. Electron Micrograph of Surface Reaction Products on Pure Iron Reacted at 900°C in 5% H_2-CH_4 for 20 Hours.
Sample No. 295 SEM 1780X

Figure 31. Electron Micrograph of Surface Reaction Products on 302 Stainless Steel Reacted at 900°C in Pure CH_4 for 20 Hours.
Sample No. 275 SEM 1780X

Figure 32. Electron Micrograph of Surface Reaction Products on 316 Stainless Steel Reacted at 900°C in 5% H_2-CH_4 for 20 Hours. Sample No. 315 SEM 1780X

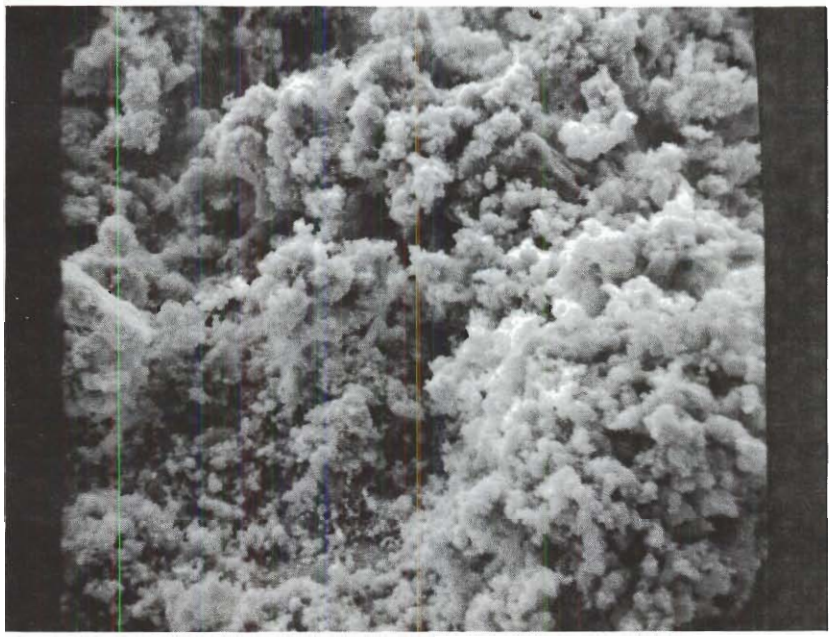

Figure 33. Electron Micrograph of Surface Reaction Products on Pure Cobalt Reacted at 880°C in 5% H_2-CH_4 for 20 Hours. Sample No. 300 SEM 1780X

Figure 34. Electron Micrograph of Surface Reaction Products on Nickel 200 Reacted at 800°C in Pure CH_4 for 20 Hours.
Sample No. 237 SEM 1780X

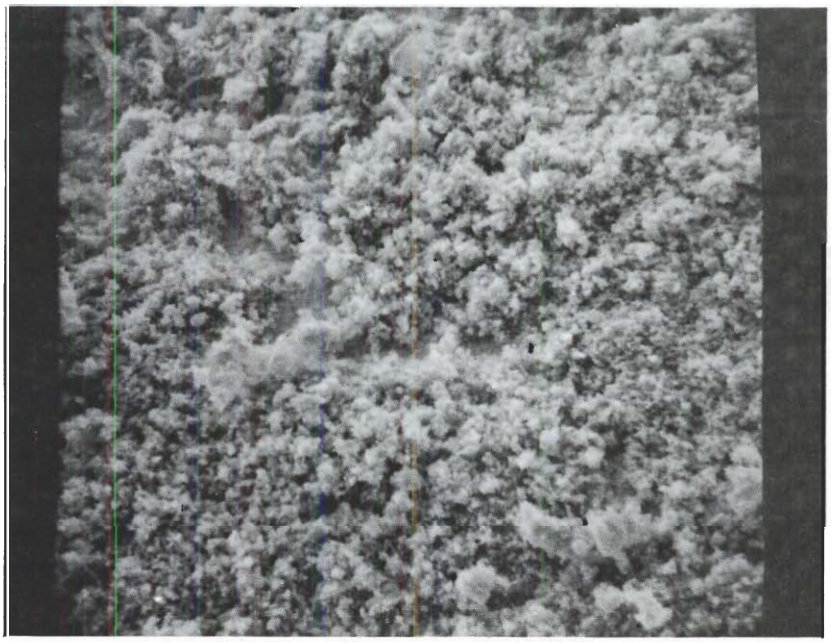

Figure 35. Electron Micrograph of Surface Reaction Products on Inconel 600 Reacted at 900°C in 5% H_2-CH_4 for 20 Hours.
Sample No. 325 SEM 1780X

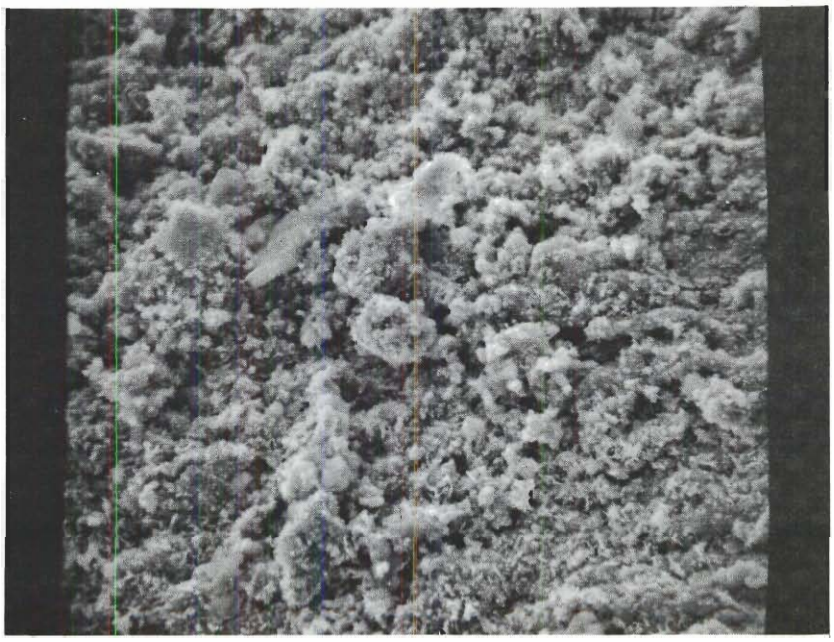

Figure 36. Electron Micrograph of Surface Reaction Products on 416 Stainless Steel Reacted at 900°C in Pure CH_4 for 20 Hours. Sample No. 285 SEM 1780X

Optical Microscopy

Microscopic examination of samples reacted in methane-hydrogen mixtures revealed information about the role of hydrogen in the reactions of the various materials with methane. Figure 37 shows the microstructure of iron after reaction with pure CH_4 at 750°C for 20 hours. Pearlite is evident throughout the sample. An iron sample exposed to a carburizing atmosphere such as CH_4 in the temperature range 723°C to 910°C experiences diffusion of carbon into the ferrite lattice forming austenite. The austenite is capable of dissolving from 0.8 to 2.0 weight per cent carbon, depending on temperature. Ferrite, in contrast, is capable of dissolving only 0.023 weight per cent carbon. Upon cooling, the austenite precipitates ferrite and cementite (pearlite) to maintain the concentration of the dissolved carbon at the saturation level of the austenite. This reasoning can be followed by observing the iron-carbon phase diagram in Figure 38.

The microstructure of iron after exposure to a 5% H_2-CH_4 mixture at 750°C for 20 hours is shown in Figure 39. This sample exhibited considerably less carburization than the sample reacted in pure CH_4. From Figure 39 it is evident that the pearlite (dark regions) formed preferentially at former austenite grain boundaries. Futhermore, it is noteworthy that the pearlite areas are near the surface of the specimen with only an isolated grain of pearlite in the center. This result is in agreement with the work of Westerman (11). It was stated earlier that samples reacted in carbon monoxide-hydrogen mixtures experienced more surface attack than samples exposed to pure carbon monoxide. Since pearlite contains 0.8% carbon and ferrite may contain only 0.023%

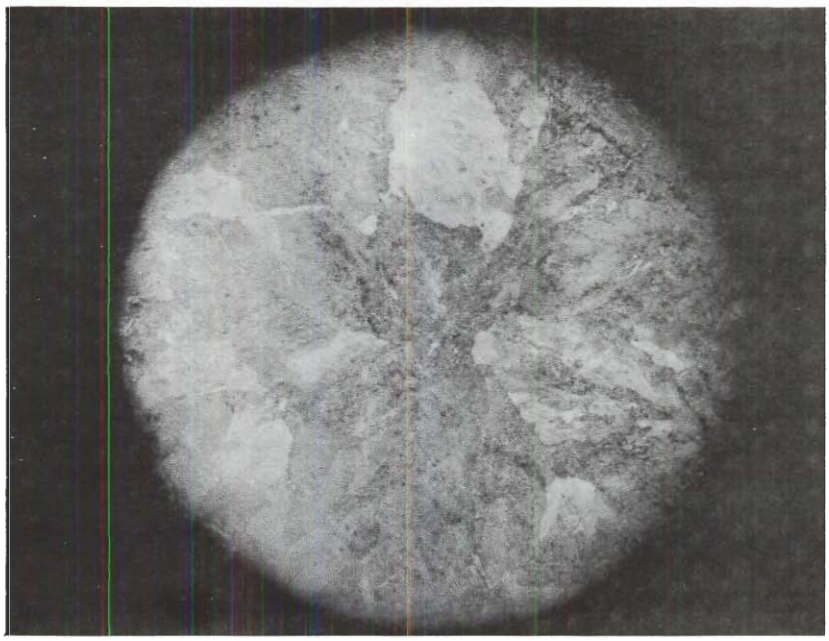

Figure 37a. The Microstructure of Pure Iron Reacted at 750°C in Pure CH_4 for 20 Hours. (Nital) Sample No. 229 150X

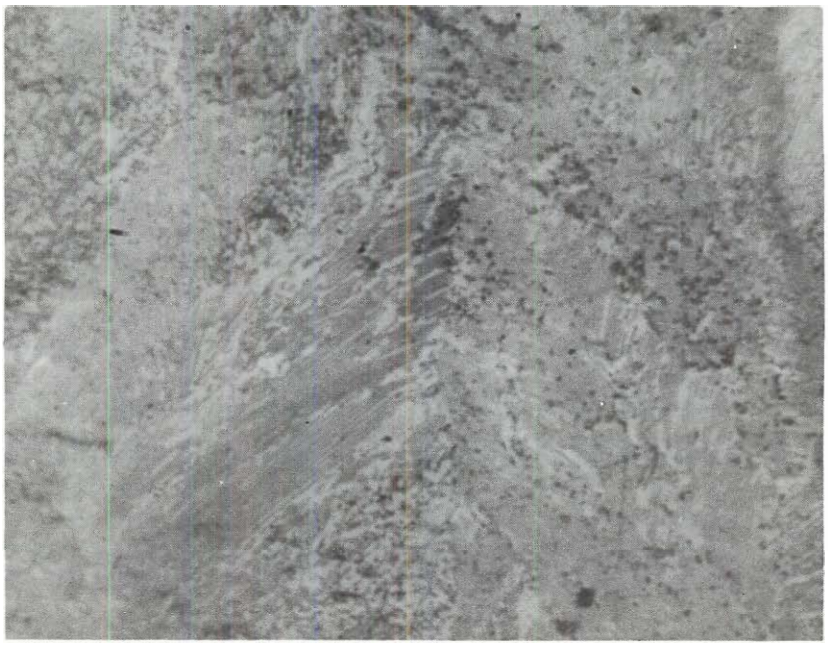

Figure 37b. The Microstructure of Pure Iron Reacted at 750°C in Pure CH_4 for 20 Hours. (Nital) Sample No. 229 1000X

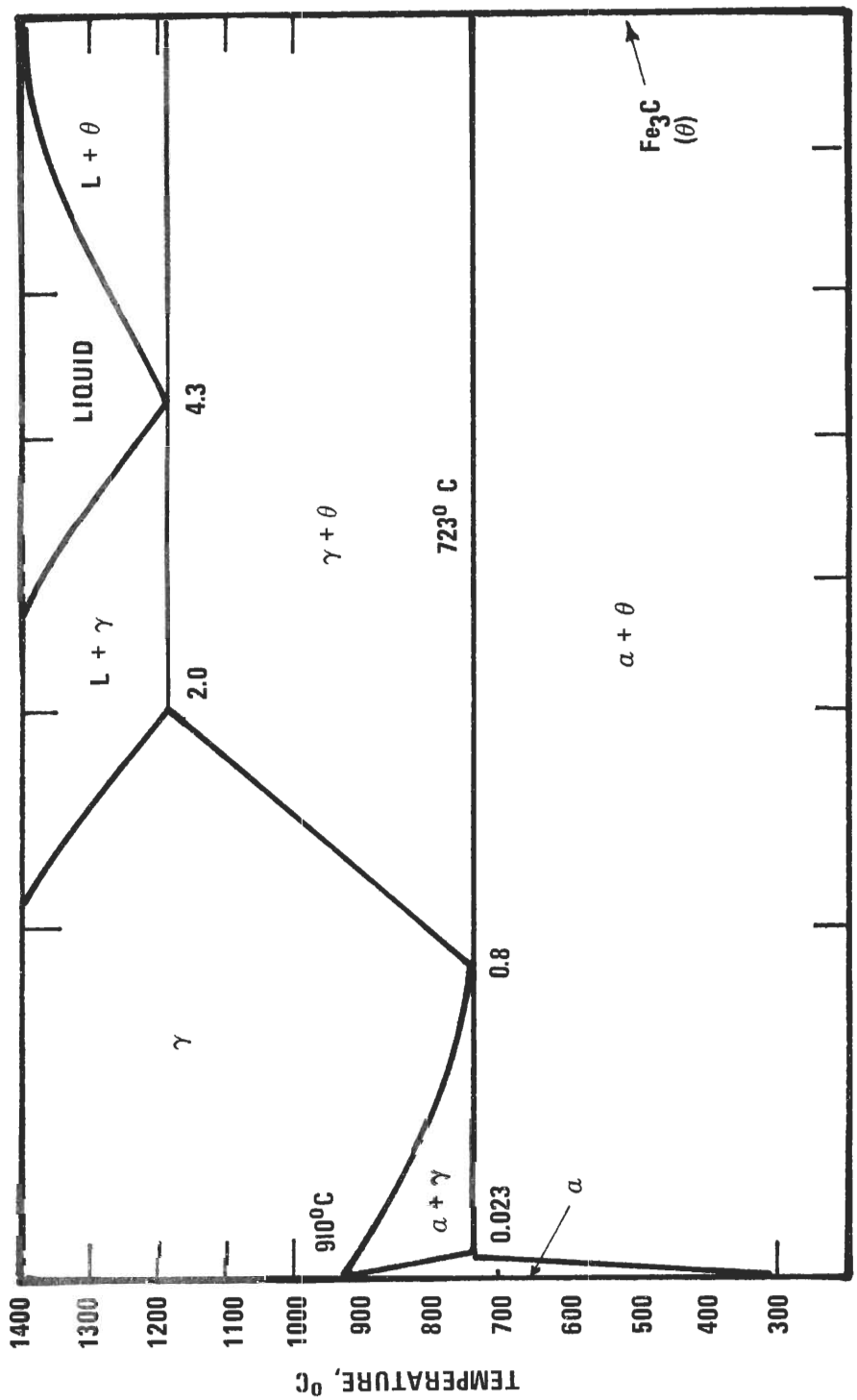

Figure 38. The Iron-Carbon Phase Diagram.

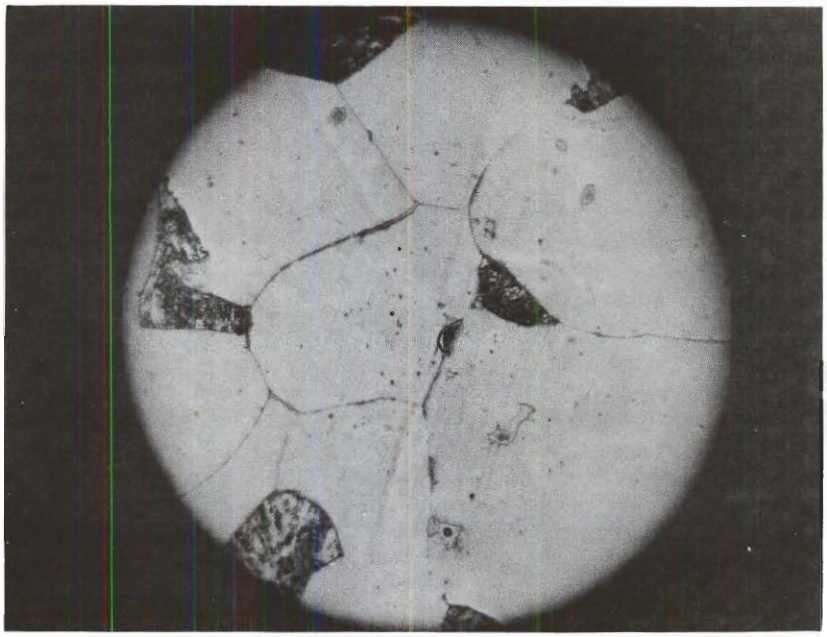

Figure 39. The Microstructure of Pure Iron Reacted at 750°C in 5% H_2-CH_4 for 20 Hours. (Nital) Sample No. 263 150X

carbon, the pearlite regions of the sample in Figure 39 represent areas of maximum carbon contant. Thus, hydrogen promotes surface attack on iron in the methane atmospheres as well as in the carbon monoxide atmospheres.

Figures 40 and 41 show the microstructures of cobalt and nickel 200, respectively, after reaction at 900°C in pure CH_4 for 20 hours. Both materials exhibited surface carburization, but to a lesser extent than the iron sample (Figure 37a). The cobalt sample has a martensitic appearance which is actually the low temperature (HCP) structure. Cobalt undergoes a lattice transformation from FCC to HCP upon cooling below 400°C.

The microstructure of 316 stainless steel after reaction at 900°C in pure CH_4 for 20 hours is shown in Figure 42. Extensive carburization and surface carbon deposition are evident. Carbide networks (Figure 42b) are prominent in the grain boundaries and throughout the grains.

Thus, the reaction of methane with the various metals and alloys is a combination of surface carbon-hydrocarbon deposition, internal carburization, and carbide formation. As in carbon monoxide environments, hydrogen in methane promotes surface attack.

Ammonia and Hydrogen Sulfide

At suitable temperatures, all steels are capable of forming stable iron nitrides in the presence of nascent nitrogen. Alloys containing one or more of the principal nitride-formers such as chromium, vanadium, molybdenum, or aluminum show exceptionally good nitriding

Figure 40. The Microstructure of Pure Cobalt Reacted at 900°C in 5% H_2-CH_4 for 20 Hours. (Nital) Sample No. 301 110X

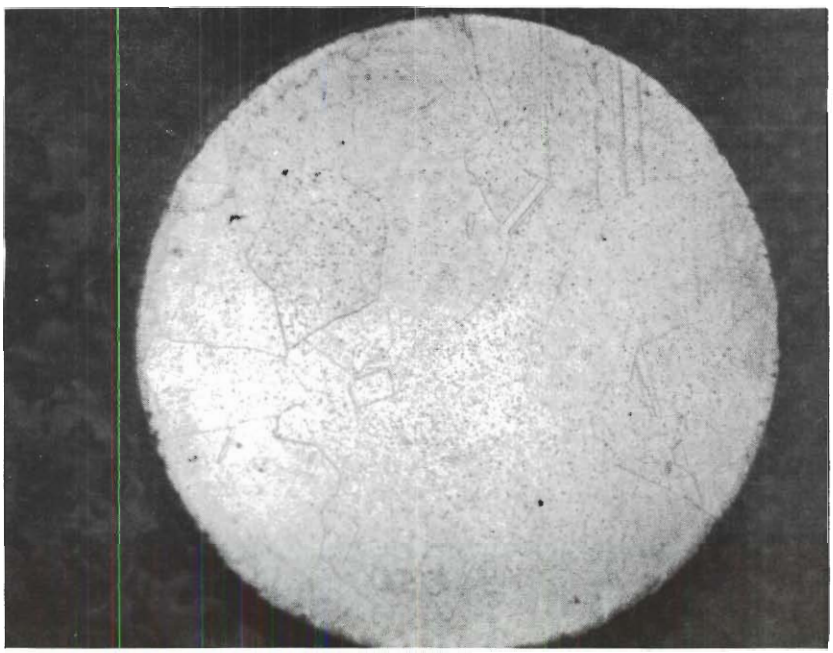

Figure 41. The Microstructure of Nickel 200 Reacted at 900°C in 5% H_2-CH_4 for 20 Hours. (Acetic/Nitric) Sample No. 305 120X

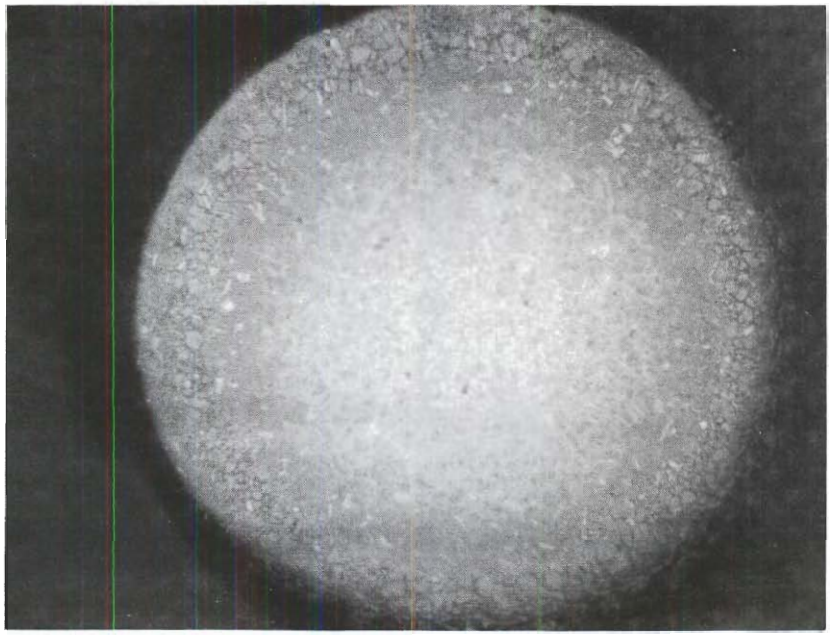

Figure 42a. The Microstructure of 316 Stainless Steel Reacted at 900°C in Pure CH_4 for 20 Hours. (Glyceregia) Sample No. 280 110X

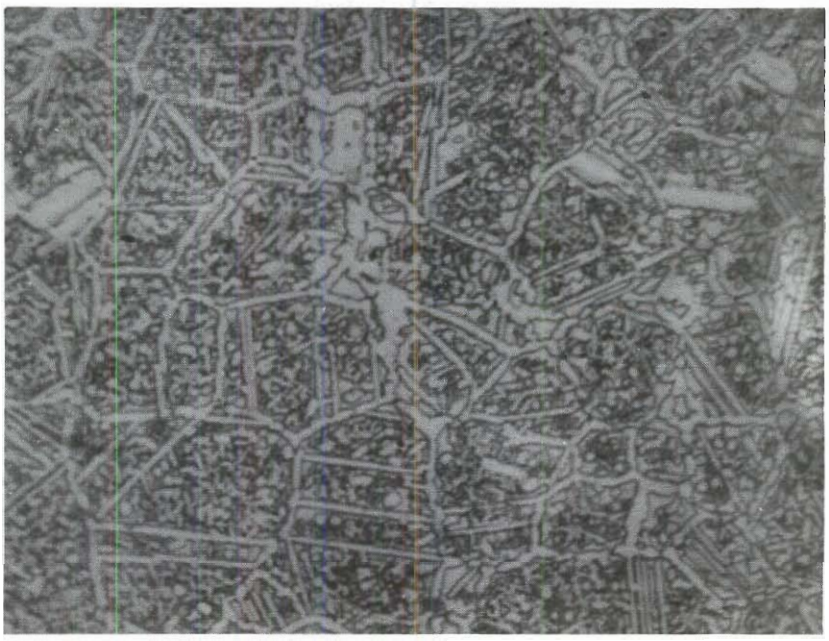

Figure 42b. The Microstructure of 316 Stainless Steel Reacted at 900°C in Pure CH_4 for 20 Hours. (Glyceregia) Sample No. 280 1000X

characteristics. Furthermore, the elements copper, silicon, manganese, and nickel appear to have little effect on the nitriding process.

Table 6 shows the effects of ammonia pretreatment on the reactivities of several materials subsequently exposed to pure carbon monoxide. Iron, 302 SS, and 316 SS showed less reactivity in pure CO after pretreatment with ammonia compared to samples not pretreated. Types 302 and 316 experienced about 50% reduction in reactivity with pretreatment while iron showed about 80% reduction. These results are consistent with the nitriding theory that predicts the formation of stable nitrides from iron, chromium, and molybdenum at nitriding temperatures. The existence of nitrides retards catalytic activity for the promotion of the Boudouard and related reactions. Hence, carbon deposition can be expected to decrease.

Nickel 200 and Inconel 600 showed more reactivity with NH_3 pretreatment than without. It is proposed that hydrogen adsorbed by the nickel served as a reducing agent for carbon monoxide decomposition. Other investigators (21) have shown that nickel-containing materials with a history of contact with hydrogen show a much greater tendency to decompose CO than nickel alloys with no such history. Since nickel nitride is metastable, it is not expected that nitrogen significantly affects the reactivity characteristics of nickel. Therefore, the increased reactivity upon ammonia pretreatment may be attributed to hydrogen adsorption following the decomposition of ammonia to hydrogen and nitrogen.

Additions of sulfur in the form of free sulfur, butyl mercaptan,

or carbon disulfide have been shown to effectively inhibit carbon deposition on ferrous alloys. Table 7 shows that hydrogen sulfide is also capable of reducing carbon formation on iron, cobalt, and type 416 stainless steel. Of these materials, iron experienced the most significant reduction in reactivity, 73%, after pretreatment with hydrogen sulfide. It is proposed that the formation of sulfide layers or adsorbed sulfur provided barriers to the adsorption of carbon monoxide and prevented CO decomposition to carbon dioxide and carbon.

Experiments with ammonia and hydrogen sulfide were of a preliminary nature and merely established the feasibility of inhibiting the metal dusting reactions by pretreatment with NH_3 or H_2S. Research to determine the optimum inhibitive conditions will be a valuable extension of this work.

Table 4. Summary of Results of Reactivity Studies for a Number of Metals and Alloys in Pure and Mixed Atmospheres

Material	Atmosphere	Experimental Temperature Range, °C	Temperature of Maximum Reactivity, °C
Fe	CO	500-850	550
Fe	5%H_2-CO	500-850	600
Fe	10%H_2-CO	500-850	500-600
Fe	CH_4	600-900	900
Fe	5%H_2-CH_4	600-900	900
Co	CO	500-850	550
Co	5%H_2-CO	500-850	550
Co	10%H_2-CO	500-850	600
Co	CH_4	600-900	750
Co	5%H_2-CH_4	600-900	880
Ni 200	CO	500-850	850
Ni 200	5%H_2-CO	500-850	625
Ni 200	10%H_2-CO	500-850	675
Ni 200	CH_4	600-900	800
Ni 200	5%H_2-CH_4	600-900	900
302 SS	CO	500-850	650
302 SS	5%H_2-CO	500-850	625
302 SS	10%H_2-CO	500-850	675
302 SS	CH_4	600-900	900
302 SS	5%H_2-CH_4	600-900	900
316 SS	CO	500-850	650
316 SS	5%H_2-CO	500-850	625-675
316 SS	10%H_2-CO	500-850	800
316 SS	CH_4	600-900	900
316 SS	5%H_2-CH_4	600-900	900
416 SS	CO	500-850	550
416 SS	5%H_2-CO	500-850	550
416 SS	10%H_2-CO	500-850	675
416 SS	CH_4	600-900	700
416 SS	5%H_2-CH_4	600-900	880
Inconel 600	CO	500-850	750
Inconel 600	5%H_2-CO	500-850	775
Inconel 600	10%H_2-CO	500-850	675
Inconel 600	CH_4	600-900	900
Inconel 600	5%H_2-CH_4	600-900	900

Table 5. Relative Reactivities of Metals and Alloys in Various Atmospheres*

CO	Max. Deposition Grams Per CM^2	5% H_2-CO	Max. Deposition Grams Per CM^2	10% H_2-CO	Max. Deposition Grams Per CM^2	CH_4	Max. Deposition Grams Per CM^2	5% H_2-CH_4	Max. Deposition Grams Per CM^2
Ni	.00024	Ni	.0017	302 SS	.00021	416 SS	.00079	416 SS	.0020
Co	.0016	Inconel 600	.0022	Inconel 600	.00066	Co	.0011	Co	.0026
416 SS	.0018	302 SS	.0023	316 SS	.00084	Fe	.0040	Ni	.0043
Inconel 600	.0019	316 SS	.0024	416 SS	.0018	316 SS	.0062	Fe	.0046
302 SS	.0028	Co	.021	Ni	.0029	Ni	.0066	302 SS	.0063
316 SS	.0053	416 SS	.077	Co	.014	302 SS	.0068	316 SS	.0063
Fe	.0069	Fe	0.43	Fe	0.18	Inconel 600	.011	Inconel 600	.014

* Note: Data are absolute maximum reactivities. Before one material is favored over another, temperature of use must be considered; e.g., 316 SS shows second highest absolute reactivity in a 5% H_2-CH_4 atmosphere, but (referring to Fig. 27) 316 shows exceptionally low reactivity below 750°C.

Table 6. Reactivities of Samples Pretreated with NH_3* Compared to Samples not Pretreated

Material	Deposition, GMS/CM^2 With Pretreatment	Deposition, GMS/CM^2 Without Pretreatment
Fe	.0010	.0048
302	.0015	.0028
316	.0026	.0053
Inconel 600	.0018	.00024
Ni 200	.00084	.000047

* Subjected to NH_3 atmosphere for 2 hours at 650°C and subsequently reacted at 650°C for 20 hours in pure CO.

Table 7. Reactivities of Samples Pretreated with H_2S* Compared to Samples not Pretreated

Material	Deposition, GMS/CM^2 With Pretreatment	Deposition, GMS/CM^2 Without Pretreatment
Fe	.0018	.0066
Co	.0016	.0017
416	.0012	.0019

* Subjected to H_2S atmosphere for 1 hour at 550°C and subsequently reacted at 550°C for 20 hours in pure CO.

CHAPTER V

CONCLUSIONS

From the research it was concluded that:

(1) Hydrogen in carbon monoxide increases carbon deposition on iron, cobalt, nickel 200, AISI 416 stainless steel, and Inconnel 600 compared to pure carbon monoxide. The hydrogen promotes production of catalytic surface for the reaction

$$2CO \rightarrow C + CO_2$$

(2) Hydrogen in carbon monoxide promotes surface attack primarily by conversion of the carbided base metal to the metal catalyst in the case of cobalt and iron-base alloys, and by adsorption on the catalytic surface in the case of nickel-base alloys. Adsorption of hydrogen without carbide formation is probably a secondary mechanism for the decomposition of carbon monoxide on cobalt and iron-base alloys.

(3) Significant reactivity of the various metals and alloys in methane occurs only at temperatures above 650°C, the minimum temperature for initiation of the thermal decomposition of methane to carbon and hydrogen.

(4) Hydrogen in methane does not affect the reactivity of methane with iron-base alloys due to equilibrium considerations of the thermal decomposition reaction

$$CH_4 \rightleftarrows C + 2H_2$$

(5) At 650°C in pure CO, ammonia pretreatment decreases the reactivities of iron and types 302 and 316 stainless steels by the formation of stable nitrides, but increases the reactivities of nickel 200 and Inconel 600 by adsorption of hydrogen which subsequently promotes the decomposition of the CO.

(6) At 550°C in pure CO, hydrogen sulfide pretreatment decreases the reactivities of iron, cobalt, and type 416 stainless steel, probably as a result of the formation of sulfide layers and adsorbed sulfur which serve as barriers to the adsorption of CO.

CHAPTER VI

RECOMMENDATIONS

Since metal dusting is not completely understood, its investigation remains of considerable interest to industry. Further studies with mixed gases in conjunction with the determination of optimum techniques for minimizing metal deterioration are areas where the extent of research is still virtually unlimited. In particular, this study revealed the following possibilities for additional research:

(1) an investigation of the basic mechanisms by which hydrogen alters the characteristics of carbon deposition on various metals and alloys in CO and CH_4 atmospheres

(2) a study to determine the effects of reaction products on the metal dusting phenomena

(3) the development of alloys which produce thermodynamically stable reaction products in CO and CH_4 environments

(4) the determination of optimum conditions for inhibiting metal deterioration with ammonia, hydrogen sulfide, water, etc.

(5) an evaluation of the metallurgical effects produced on metals and alloys by various inhibiting techniques.

APPENDICES

APPENDIX A

MATERIAL CHARACTERISTICS

Table 8. Wire Sample Characteristics

Material	Wire O. D. (inches)	Wire O. D. (cm.)	Wire Length* (cm.)	Typical Coil O. D. (cm.)
316 SS	0.0348	0.0884	36.1	0.320
302 SS	0.025	0.064	50.2	0.310
Nickel 200	0.025	0.064	50.2	0.305
Inconel 600	0.025	0.064	50.2	0.315
Cobalt	0.020	0.051	62.7	0.350
Iron	0.020	0.051	62.7	0.340
416 SS	0.015	0.038	83.8	0.335

* Length to yield 10 cm^2 surface area.

Table 9. Chemical Compositions of Wire Samples

Material	Elements									
	Co	Ni	C	Mn	Fe	Si	Cu	Cr	Mo	S
316 SS		10-14	0.08 max	2.00 max	Bal	1.00 max		16-18	2-3	
302 SS		8-10	0.15 max	2.00 max	Bal	1.00 max		17-19		
Nickel 200		99.5	0.06	0.25	0.15	0.05	0.05			
Inconel 600		76.4*	0.04	0.20	7.20	0.20	0.10	15.85		
Cobalt	99.9									
Iron					99.99					
416 SS			0.15 max	1.25 max	Bal	1.00 max		12-14		0.15 max

* Includes cobalt

Table 10. Gas Characteristics

Material	Supplier	Description
CO	Matheson Co.	C. P. grade
$CO-5\%H_2$	Linde Division Union Carbide	Specialty gas
$CO-10\%H_2$	Linde Division Union Carbide	Specialty gas
CH_4	Matheson Co.	Ultra high purity
$CH_4-5\%H_2$	Linde Division Union Carbide	Specialty gas

APPENDIX B

THE SCANNING ELECTRON MICROSCOPE

Uses and Advantages

Surface features which are difficult to examine by conventional optical or electron microscope techniques are ideally suited for study with the scanning electron microscope. The instrument is also useful for the investigation of fracture surfaces and powder characteristics. Samples need not be metallic since vapor depositing a thin layer of metal on non-metallic specimens prevents them from being charged by the electron beam. Other than the vapor depositing step for non-metallics, no sample preparation is required. Besides the ease of sample preparation, other advantages of the scanning electron technique include good resolution (150 Å), exceptional depth of focus (about 300 times that of an optical microscope), rapid instrument operation, and ease of image interpretation.

Operation

A specimen bombarded with high energy electrons emits back-scattered electrons, secondary electrons, and x-rays. Selective analysis of the emitted particles provides useful information about the sample. The electron microprobe, for example, relies on the characteristic x-ray flourescence of materials for its elemental analysis.

Secondary and backscattered electrons provide information about surfaces. High energy backscattered electrons move from the sample to the collector in a straight line. The lower energy secondary electrons follow a curved path to the collector and reveal details of holes, crevices, etc. The electron beam is accelerated from 20 to 25 kv. Condenser and objective lenses focus the beam on the specimen surface from which electrons are emitted. Electrons collected in the detector comprise a signal which is amplified and displayed on a cathode ray tube.

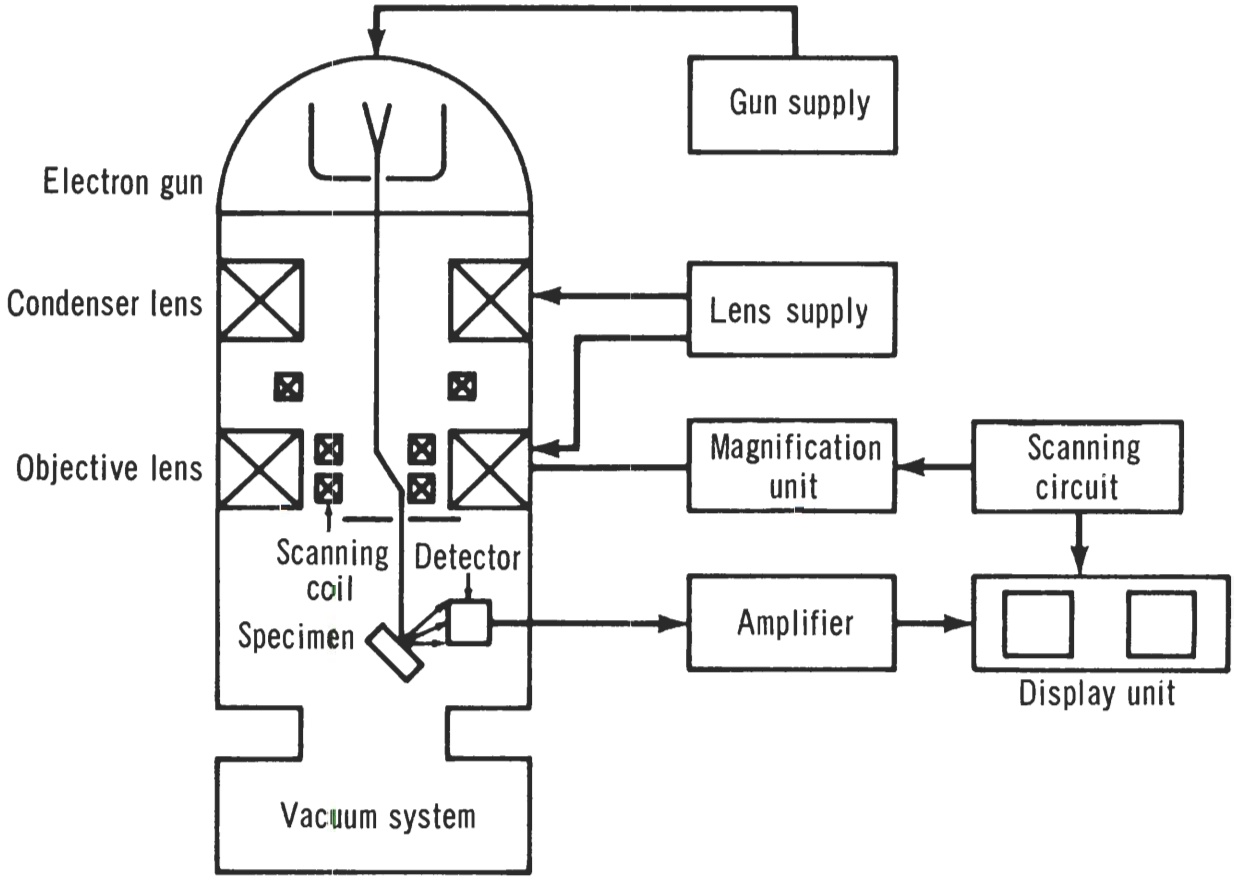

Figure 43. Schematic of the Scanning Electron Microscope.

APPENDIX C

BIBLIOGRAPHY*

Literature Cited

1. Walker, P. L., Rakszawski, J. F., and Imperial, G. R., "Carbon Formation from Carbon Monoxide-Hydrogen Mixtures over Iron Catalysts," J. Phys. Chem. 63, 133-140 (1959).

2. B.I.O.S. Final Report No. 1399, Item No. 22.

3. French Patent No. 874,681 (August 18, 1942).

4. U.S. Patent No. 2,716,053 (August 23, 1955).

5. Hochman, R. F., Metal Deterioration in High Temperature Carbonaceous Environments, Annual Report 1, National Association of Corrosion Engineers, p. 4 (1966).

6. Everett, M. R., "The Kinetics of Carbon Deposition Reactions in High Temperature Gas Cooled Reactors," Internal Dragon Report, 1967.

7. Das, P. P., and Chattergee, B., Trans. Ind. Inst. Metals 6, 279 (1952).

8. Rischbieth, P., Z. Phyzik. Chem. Unterricht 44, 22-24 (1931).

9. Drain, Jean, "A Physical-Chemical Study of Carburized Phases of Cobalt and of Some Special Cementites," Ann. Chim. (Paris) 8, 900-953 (1954).

10. Berry, T. F., Ames, R. N., and Snow, R. B., J. Am. Cer. Soc. 39, 308 (1956).

11. Westerman, R. V., The Mechanism and Kinetics of Iron Deterioration in Carbon Monoxide, Ph.D. Thesis, Georgia Institute of Technology, Atlanta, Georgia, 1968.

12. Hofer, L. J. E., Catalysis, Vol. 4, New York: Reinhold Publishing Corp., 373-441 (1956).

---

* The abbreviations in this Bibliography follow the form used in Chemical Abstracts (1965).

13. Hoyt, W. B. and Caughey, R. H., "High Temperature Metal Deterioration in Atmospheres Containing Carbon Monoxide and Hydrogen," Corrosion 15, No. 12, 627t (1959).

14. Segraves, W. B., Corrosion of Nickel Containing Materials by Carbon Monoxide at Elevated Temperatures, Ph.D. Thesis, Georgia Institute of Technology, Atlanta, Georgia, 1960.

15. Phillips, C., Cross, L., and Camp, E., "Corrosion of 18-8 Alloy Furnace Tubes in High-Temperature Vapor Phase Cracking Service," Corrosion 1, 149 (1945).

16. Burns, O. L., "Corrosion on a New Distillation Unit Processing Low Sulfur Crude," Corrosion 6, 169 (1950).

17. Merrick, R. D., "High Temperature Furnace Corrosion of Type 309 Alloy Steel," Corrosion 16, 578t (1960).

18. Hopkinson, Copson, "Internal Carburization and Oxidation of Nickel-Chromium Alloys in Carbon Monoxide Type Atmospheres," Corrosion 16, 608t (1960).

19. Hubbell, W. G., "Carbon Absorption of 18-8 Stainless Steel," The Iron Age 56, 157 (1946).

20. Prange, F. A., "Corrosion in a Hydrocarbon Conversion System," Paper No. 13, Fifteenth Annual Conference of the National Association of Corrosion Engineers, Chicago, Illinois, (March 16-20, 1959).

21. Cox, A. R., The High-Temperature Reactions of Carbon Monoxide with Iron, Nickel, and Austenitic Stainless Steel, M. S. Thesis, Georgia Institute of Technology, 1962.

22. Kehrer, V. J. and Leidheiser, H., "The Catalytic Decomposition of Carbon Monoxide on Large Metallic Single Crystals," J. Phys. Chem. 58, 550-555 (1954).

23. Grenga, H. E., Active Sites for the Catalytic Decomposition of Carbon Monoxide on Nickel, Ph.D. Dissertation, University of Virginia, 1967.

24. Skinner, E. N. and Raudebaugh, R. J., The Deteriorating Effect of Carbon Monoxide on Certain Alloys at 1050°F, Development and Research Division, International Nickel Co., New York, 1958.

25. Eberle, F. T. and Wylie, R. D., "Attack on Metals by Synthesis Gas from Methane-Oxygen Combustion," Corrosion 15, 622t-626t (1959).

26. Prange, F. G., "Dusting in Butane Dehydrogenation Service," Corrosion 15, 619t (1959).

27. Baukloh, W. and Hieber, G., "Der Einfluss Verschiedener Metalle und Metalloxyde auf die Kohlenoxydspaltung," Zeitschrift Für Anorganische und Allegemeine Chemie 226, Part 4, 321-332 (1936).

28. Hochman, R. F., Metal Deterioration in High Temperature Carbonaceous Environments, Quarterly Progress Letter No. 1 (to N.A.C.E.) Third Project Year, Sept. 1, 1966.

29. Hochman, R. F., Metal Deterioration in High Temperature Carbonaceous Environments, Quarterly Progress Letter No. 2 (to N.A.C.E.) Third Project Year, Sept. 15, 1966.

30. Pattinson, J., "On Carbon and Other Deposits from Gases of Blast Furnaces in Cleveland," J. Iron Steel Inst. 10, 85 (1876).

31. Shea, J. A., "Treatment of Brick to Prevent Carbon Monoxide Disintegration," Iron and Steel Engr. 27, No. 12, 116-119 (1950).

32. Baukloh, W. and Henke, G., Metallwirtschaft 19, 463 (1940).

33. Klemantaski, S., J. Iron Steel Inst. (London) 171, 176 (1952).

34. Hochman, R. F., Georgia Institute of Technology, Private Communication.

35. Bone, W. A., Saunders, H. L., and Tress, H. J., J. Iron Steel Inst. (London) 137, 85 (1938).

36. Chem. Eng. News 40 (16), 68-69 (1962).

37. Hydrocarbon Process Petroleum Refiner 43 (9), 232 (1964).

38. Le Paige de Dommartin, J. L. M., "Catalytic Polymerization of Hydrocarbons," French Patent 994,031, Nov. 9, 1951.

39. Hochman, R. G., Metal Deterioration in High Temperature Carbonaceous Gas Environments, Quarterly Progress Letter No. 2 (to N.A.C.E.) Second Project Year, Sept. 1, 1965.

Other References

1. Hochman, R. F., Burson, J. H., "The Fundamentals of Metal Dusting," Proceedings of the American Petroleum Institute, Section III, 46, 331-334 (1966).

2. Dushman, S., Scientific Foundations of Vacuum Technique, 2nd Edition, J. Wiley & Sons, 752 (1962).

3. Rayet, R., Juliard, A., and Lude, A., "A Kinetic Study of the Dissociation of Carbon Monoxide Accompanying the Reduction of Metallic Oxides," Discussions Faraday Society, No. 4, translated by J. H. E. Jeffes, 193-196 (1948).